Atmospheric Environment 152 (2017) 123–145

Contents lists available at ScienceDirect

Atmospheric Environment

journal homepage: www.elsevier.com/locate/atmosenv

# Responses of human health and vegetation exposure metrics to changes in ozone concentration distributions in the European Union, United States, and China

Allen S. Lefohn [a, *], Christopher S. Malley [b], Heather Simon [c], Benjamin Wells [c], Xiaobin Xu [d], Li Zhang [e], Tao Wang [e]

[a] A.S.L. & Associates, 302 North Last Chance Gulch, Helena, MT 59601, USA
[b] Stockholm Environment Institute, Environment Department, University of York, York, YO10 5DD, UK
[c] Office of Air Quality Planning and Standards, U.S. EPA, Research Triangle Park, NC 27711, USA
[d] Key Laboratory for Atmospheric Chemistry, Institute of Atmospheric Composition, Chinese Academy of Meteorological Sciences, Zhongguancun Nandajie 46, Beijing 100081, China
[e] Department of Civil and Environmental Engineering, The Hong Kong Polytechnic University, Hong Kong, China

## HIGHLIGHTS

- Emissions changes caused shifts in distributions of $O_3$ hourly concentrations.
- At most EU and US sites, high and low concentrations shifted toward the center.
- In China concentrations shifted upwards and metrics increased or showed no trend.
- Trends in metrics were not always in same direction as regional emissions changes.
- Trends in mean or median values do not reflect trends in some effects metrics.

## GRAPHICAL ABSTRACT

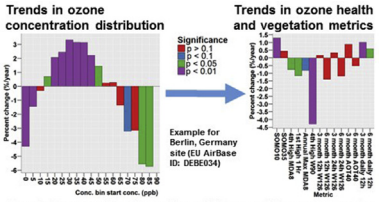


Trends in ozone health and vegetation metrics may vary for an identical change in ozone concentration distribution.

## ARTICLE INFO

*Article history:*
Received 19 September 2016
Received in revised form
8 December 2016
Accepted 10 December 2016
Available online 12 December 2016

*Keywords:*
Binning concentrations
Exposure metrics
Ozone distributions
NOx scavenging
Shifting concentrations
Trends

## ABSTRACT

The impacts of surface ozone ($O_3$) on human health and vegetation have prompted $O_3$ precursor emission reductions in the European Union (EU) and United States (US). In contrast, until recently, emissions have increased in East Asia and most strongly in China. As emissions change, the distribution of hourly $O_3$ concentrations also changes, as do the values of exposure metrics. The distribution changes can result in the exposure metric trend patterns changing in a similar direction as trends in emissions (e.g., metrics increase as emissions increase) or, in some cases, in opposite directions. This study, using data from 481 sites (276 in the EU, 196 in the US, and 9 in China), investigates the response of 14 human health and vegetation $O_3$ exposure metrics to changes in hourly $O_3$ concentration distributions over time. At a majority of EU and US sites, there was a reduction in the frequency of both relatively high and low hourly average $O_3$ concentrations. In contrast, for some sites in mainland China and Hong Kong, the middle of the distribution shifted upwards but the low end did not change and for other sites, the entire distribution shifted upwards. The responses of the 14 metrics to these changes at the EU, US, and Chinese sites were varied, and dependent on (1) the extent to which the metric was determined by relatively high,

* Corresponding author.
*E-mail addresses:* alefohn@asl-associates.com (A.S. Lefohn), malley.chris@gmail.com (C.S. Malley), simon.heather@epa.gov (H. Simon), Wells.Benjamin@epamail.epa.gov (B. Wells), xuxb@camscma.cn (X. Xu), alex.zhang@connect.polyu.hk (L. Zhang), tao.wang@polyu.edu.hk (T. Wang).

http://dx.doi.org/10.1016/j.atmosenv.2016.12.025

moderate, and low concentrations and (2) the relative magnitude of the shifts occurring within the $O_3$ concentration distribution. For example, the majority of the EU and US sites experienced decreasing trends in the magnitude of those metrics associated with higher concentrations. For the sites in China, all of the metrics either increased or had no trends. In contrast, there were a greater number of sites that had no trend for those metrics determined by a combination of moderate and high $O_3$ concentrations. A result of our analyses is that trends in mean or median concentrations did not appear to be well associated with some exposure metrics applicable for assessing human health or vegetation effects. The identification of shifting patterns in the $O_3$ distribution and the resulting changes in $O_3$ exposure metrics across regions with large emission increases and decreases is an important step in examining the linkage between emissions and exposure metric trends. The results provide insight into the utility of using specific exposure metrics for assessing emission control strategies.



## 1. Introduction

Surface ozone ($O_3$) is a secondary pollutant detrimental to human health and vegetation (CLRTAP Convention, 2015; REVIHAAP, 2013; US EPA, 2013; US EPA, 2014a). In an attempt to reduce $O_3$ levels, many countries have implemented strategies directed at reducing emissions of $O_3$ precursors (nitrogen oxides ($NO_x$) and volatile organic compounds (VOCs)). Scientists and regulators use a variety of exposure and dose metrics to establish standards for the protection of human health and vegetation, and to evaluate the effectiveness of mitigation strategies.

Substantial reductions in $O_3$ precursors have occurred in the United States (US) and European Union (EU) over the past several decades (Vautard et al., 2006; Torseth et al., 2012; Xing et al., 2013; Lu et al., 2015; Lamsal et al., 2015; Monks et al., 2015; Duncan et al., 2016). The United States Environmental Protection Agency (US EPA) began to regulate $O_3$ with the promulgation of a ground-level National Ambient Air Quality Standard (NAAQS) in 1971, with subsequent revisions in 1979, 1997, 2008, and 2015. Following promulgation of the 1997 $O_3$ standard, the US EPA issued a NOx State Implementation Plan (SIP) Call, which reduced regional summertime NOx emissions from power plants and other large stationary sources by 57% in 22 Eastern US states. In addition, the US EPA established national rules that substantially reduced NOx and VOC emissions from on-road mobile sources by 53% and 77% between 1990 and 2014, respectively (US EPA, 2015). Overall, NOx and VOC have decreased in the US by 52% and 39% from all sources since 1990 (US EPA, 2015). Similarly, the European Union 28 (EU-28) countries also targeted NOx and VOC emissions, which were reduced by 54% and 59%, respectively between 1990 and 2013 (EEA, 2015). The emission reductions across EU countries result in part from national 'emission ceilings' specified in the 1999 Gothenburg Protocol to abate acidification, eutrophication and ground-level $O_3$ (UNECE, 1999, 2013), within the UNECE Convention on Long-Range Transboundary Air Pollution (UNECE, 1979; Maas and Grennfelt, 2016).

In contrast, emissions have increased in East Asia (Streets et al., 2001; Granier et al., 2011), and most strongly in China (Streets et al., 2001; Richter et al., 2005; Ohara et al., 2007; Mijling et al., 2013; Kurokawa et al., 2013). In China, anthropogenic NOx emissions rose from about 11.0 million tons (Mt) in 1995 to 26.1 Mt in 2010, driven by the fast growth of energy consumption, with a high annual increase rate reaching up to 5.9% (Zhao et al., 2013). However, there is evidence that $NO_x$ emissions peaked in China around 2010–2011, and have started to decrease (Zhao et al., 2013; Duncan et al., 2016; Krotkov et al., 2016). The National Bureau of Statistics of the People's Republic of China (http://data.stats.gov.cn/) reports that annual NOx emissions in mainland China decreased from 24.04 Mt in 2011 to 20.78 Mt in 2014. Annual VOC emissions in China have also increased (e.g., from 6.8 Mt in 1980 to 17.2 Mt in 2003 (Ohara et al., 2007)). The evidence for regional NOx and VOC emissions trends in more recent years is mixed (Multi-resolution Emission Inventory for China; Wang et al., 2015; De Smedt et al., 2015; Sun et al., 2016). Over the Pearl River Delta (PRD) region, total NOx and VOCs emissions also increased during the 2000–2009 period (i.e., 96% and 58%, respectively) (Lu et al., 2013), but decreased by 28% and 65%, respectively in Hong Kong (located within PRD) between 1997 and 2014 due to implementation of local government control policies (http://www.epd.gov.hk/).

Changes in the magnitude of national and regional emissions described above, as well as any long-term changes in international emissions, climate, and inter-annual meteorological variability, can drive shifts in the distributions of hourly surface $O_3$ concentrations. While VOC emission reductions generally lead to corresponding decreases in $O_3$, the response of $O_3$ to NOx reductions is more variable as NOx participates in both $O_3$ formation and destruction chemical pathways. Many studies have characterized the $O_3$ production efficiency (OPE), defined as the number of $O_3$ molecules produced by each NOx molecule (Liu et al., 1987), for different times and locations. OPE generally increases as total VOC/NOx ratios, VOC reactivity, and UV insolation increase (Lin et al., 1988; Liu et al., 1987; Sillman, 1990; Sillman et al., 1990; Walcek and Yuan, 1995). Conversely, in conditions where the VOC/NOx ratio is low or where there is relatively little UV insolation (VOC limited or NOx saturated conditions), NOx can result in net destruction of $O_3$. VOC limited conditions often also coincide with lower $O_3$ concentrations due to low chemical production of $O_3$ (i.e., resulting from low amounts of UV or less reactive VOC) and substantial $O_3$ destructions from NOx scavenging. Consequently, the impacts of NOx reductions on $O_3$ concentrations may be spatially and temporally varying, leading to $O_3$ increases at times and locations where $O_3$ is low (e.g., at night, during winter, during summer days with less insolation, and at times and locations with high magnitudes of fresh NO emissions) and $O_3$ decreases at times and locations where $O_3$ is high (e.g., in the afternoon, during summer days with the highest UV fluxes, and at locations downwind of large NO sources). As a result, when NOx emissions are reduced, low $O_3$ concentrations often shift upwards, while high concentrations shift downward (US EPA, 2014a).

Changes in the distributions of hourly average $O_3$ concentrations can result in changes in the magnitude of exposure metrics used for assessing human health and vegetation effects. However, trend patterns in $O_3$ exposure metrics may be in a similar direction as emissions changes (e.g., metrics increase as emissions increase) or may not (Karlsson et al., 2007; EEA, 2009; Tripathi et al., 2012; Li et al., 2014; Paoletti et al., 2014; Simpson et al., 2014; Malley et al., 2015; Sicard et al., 2016).

Over the past 20–30 years, substantial changes in $O_3$ concentrations have been observed at many sites across the world, likely

driven by a combination of the large emissions changes discussed above (both locally and in upwind regions) and potentially by shifts in various meteorological conditions. In this analysis, we aim to better understand the relationship between exposure metrics, hourly $O_3$ concentration distributions, and emission changes. To achieve this, we analyze the response of 14 human health and vegetation $O_3$ metrics to long-term changes in the hourly $O_3$ concentration distribution, as measured at 481 monitoring sites in the EU, US, and China. The sites represent a variety of conditions (e.g., site classification, altitude, proximity to emission sources, influence of long-range transport, etc.), and the three regions have contrasting long-term trends in $O_3$ precursor emissions. This allows the assessment of the behavior of these metrics across a wide range of conditions. The identification of shifting patterns in the $O_3$ distribution and the resulting changes in $O_3$ exposure metrics across regions with large emission increases and decreases is an important step towards creating a universally applicable understanding of the linkage between emissions and exposure metric trends. This study further provides insight into the utility of using specific exposure metrics for assessing emission control strategies.

## 2. Approach

First, patterns of changes in the hourly average $O_3$ concentration distributions across a diverse range of surface $O_3$ monitoring sites were characterized. Multi-year trends were then calculated for a set of exposure metrics used for assessing human health and vegetation effects. The relationships between exposure metric trends and the changing $O_3$ distribution patterns were described and the underlying causes for these relationships were investigated.

### 2.1. Site selection, trend time period, and data processing

We assessed trends over sufficient time periods (i.e., with a minimum of 20 years) so that the trend signal would be more easily distinguishable from the inter-annual $O_3$ variability. The specific criteria used to determine inclusion of EU and US sites in this analysis are detailed in Section 2.1.1 and 2.1.2 below. However, as noted above all sites included in these regions had a monitoring record of at least 20 years. While this criterion allowed inclusion of a large number of EU and US sites, a lack of data for several of the sites in China resulted in using data over a shorter time period to characterize trends. While data quality protocols may be different among the three regions, the quality of the data in each database met the requirements established by each country/region. In addition, the time period over which trend analyses were conducted also varied between sites to make use of the maximum monitoring record at each site. At many sites this approach allowed the assessment of changes in $O_3$ concentration distribution, and response of health and vegetation metrics to be undertaken over a period with larger changes in $O_3$ precursor emissions than would have been possible using a fixed time period applied across all sites.

#### 2.1.1. EU

Publicly available $O_3$ time series data were obtained from the EU AirBase data repository (http://www.eea.europa.eu/data-and-maps/data/aqereporting) for all sites with continuous, year-round measurements covering at least 20 years (1994–2013). The last year of record in the EU database included in our analyses was 2013. Monitoring sites which collected data as far back as 1981 were included in the study. In total, 276 sites in 11 European countries met this criterion and were included in the analysis (Fig. 1a and Table 1). At 87% of these sites, the longest gap in $O_3$ measurements was less than 1 year, but sites with longer data gaps were included to maximize the number of sites. Less than 8% of sites had more than 2 years with missing data. The sites in AirBase, with a sufficient time period, were not evenly distributed across the EU, and there were few sites selected in southern and Eastern Europe. The terminology used to classify sites in the EU is based on an assessment of the 'type of area' and the 'type of station'. The former refers to the environment on the scale of several kilometers and is assigned urban (continuously built up urban area), suburban (largely built up urban area but building density is lower than urban area), or rural. The type of station refers to the impact of nearby emissions, and is characterized as traffic (site located in close proximity to a major road), industrial (close proximity to an industrial source), or background (i.e., does not fulfill criteria for traffic or industrial and pollutant concentrations that are representative of the average for the type of area (European Commission, 2013; JRC-AQUILA, 2013)). Different combinations of area type and station type therefore result in different classifications (e.g., rural background, suburban background, urban background, urban traffic, and urban industrial). Table 1 provides a summary of the numbers in each category.

#### 2.1.2. US

The US EPA maintains the Air Quality System (AQS) database (www.epa.gov/aqs), which contains air pollutant concentration data reported by state, local, and tribal agencies. Hourly $O_3$ concentration data are currently reported to AQS from over 1200 $O_3$ monitoring sites nationwide. For the purpose of this analysis, the following criteria were used to select sites: (1) sites that collected data with a minimum of 20 years (1995–2014) but including those sites initiating monitoring as far back as 1980; (2) sites that collected data year-round over the entire period; and (3) sites that did not experience large data gaps in the monitoring record with more than one large data gap of up to 1 year in length.

The second criterion was applied because many $O_3$ monitoring sites in the US do not operate year-round. Since the distribution of $O_3$ values and their response to emissions changes vary by season (Cooper et al., 2010; Simon et al., 2015; Clifton et al., 2014), trends at partial-year monitors may not be fully representative. In addition, several of the exposure metrics evaluated in this analysis are calculated using varying 3- and 6-month periods making it important to include only monitoring sites collecting data year-round.

US sites covered urban, suburban, and rural locations as defined by Simon et al. (2015) using the 2006 National Land Cover Database (NLCD). The majority of "urban" monitors in the subset of US sites were located in California. In order to include more urban monitors across the US, the first criterion was relaxed to include some urban sites whose data records began as late as 1995. With this relaxation, 12 urban sites were added to the analysis (i.e., two in Colorado, two in Illinois, four in Pennsylvania, three in Texas, and one in Louisiana). A total of 196 monitoring sites across the contiguous US were included in the study (Fig. 1b and Table 2).

In the US, $O_3$ data are reported to the AQS at 1 ppb precision. However, historically some state and local monitoring agencies reported $O_3$ data to the AQS at 10 ppb precision. A large fraction (~40%) of the sites included in the analysis used the 10 ppb reporting convention until the mid-1990s. In order to allow all hourly $O_3$ data to be classified into 5 ppb bins (see Section 2.3), artificial scatter was added to the 10 ppb precision data. For each monitoring site, we identified any months for which all hourly $O_3$ concentration values ended in 0. For those months, a random value drawn from a Discrete Uniform distribution with a minimum of -5 ppb and a maximum of 5 ppb was added to each hourly $O_3$ concentration. Supplement Appendix D describes an analysis which examined the impact of the low precision data and associated artificial scatter data on trends in $O_3$ exposure metrics. While

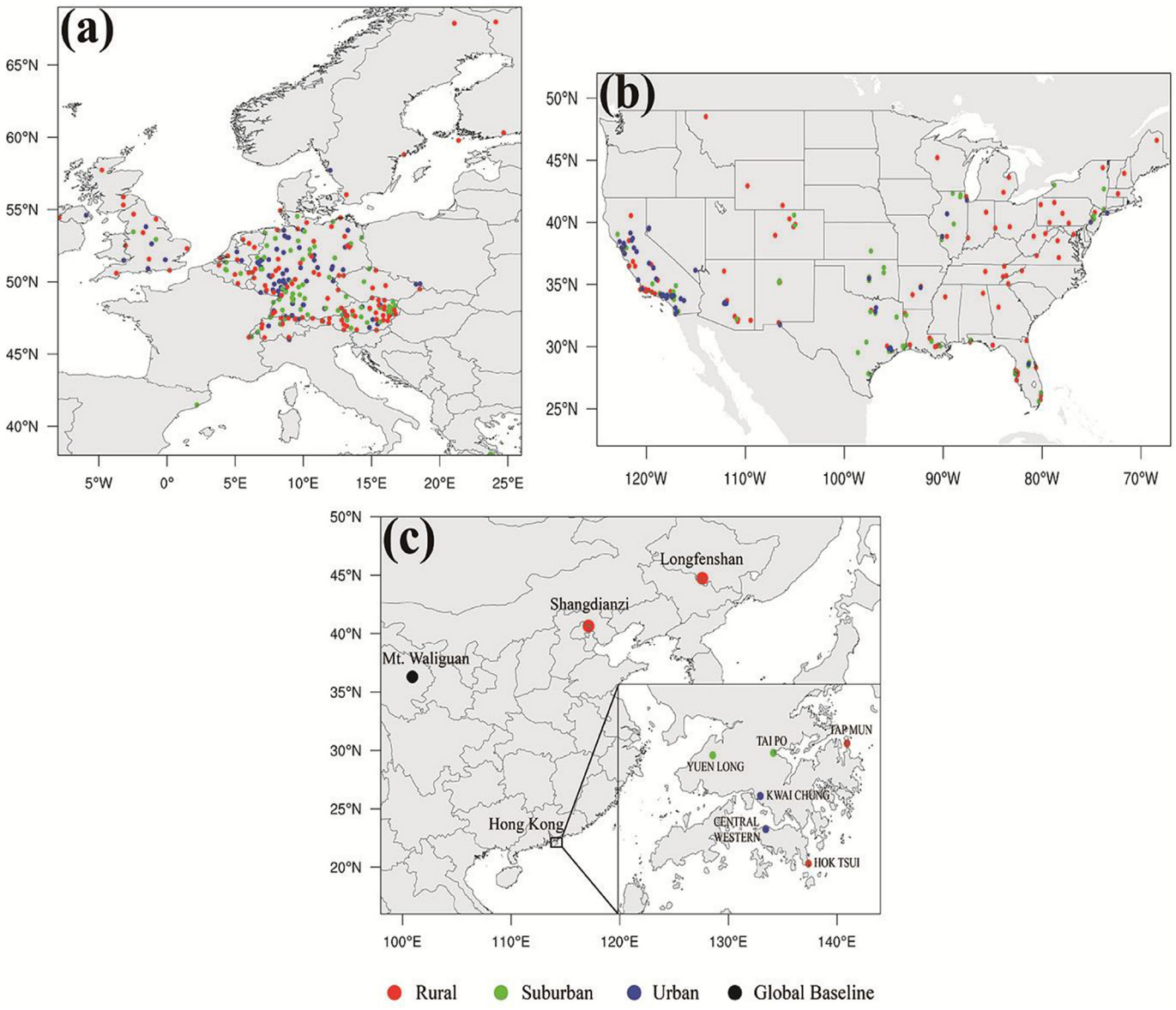


**Fig. 1.** Map of (a) EU, (b) US, and (c) mainland China and Hong Kong, China sites selected for the study.

the change from low to higher precision reporting had a small impact on the exposure metric trends, the artificial scatter did not create additional bias in these trends.

### 2.1.3. China

For this analysis, we report trends from three sites in mainland China and six sites in Hong Kong (Special Administrative Region) (Fig. 1c and Table 3). Hourly average $O_3$ data collected over an extended period (i.e., greater than 20 years) in China are scarce. Besides monitoring sites in Hong Kong, only one site in mainland China collected data over a 20-year period (i.e., Mt. Waliguan, Qinghai Province, 1994–2015). Two additional sites from mainland China (Shangdianzi, Beijing, Capital City and Longfengshan, Heilongjiang Province) were included in the study (Fig. 1c). Although the Mt. Waliguan site began monitoring in 1994, data capture considerations resulted in trends analyses being performed over the 2000–2015 period. Similarly, for the Longfengshan site, although data existed for 2005, the 2006–2015 period was used in the trends analyses.

The Mt. Waliguan site, established in 1994, is situated at the northeastern edge of the Tibetan Plateau (Xu et al., 2016). It is a global baseline site within the World Meteorological Organization's Global Atmosphere Watch (WMO/GAW) network. Surface $O_3$ at the site is highly representative of free-tropospheric $O_3$ (Ma et al., 2002) and is often influenced by stratosphere-to-troposphere transport (STT) events (Ding and Wang, 2006; Zhu et al., 2004). Air masses from the west are dominant at Mt. Waliguan and are associated with the highest $O_3$ concentrations (Wang et al., 2006). The site is far from major cities, such as Xining (90 km) and Lanzhou (260 km) in the eastern sector. During the summer, surface $O_3$ concentrations may be subject to regional anthropogenic influences from the eastern sector (Wang et al., 2006; Xue et al., 2011). According to China's national statistics (http://data.stats.gov.cn/), NOx emissions in Qinghai province, in which Mt. Waliguan is located, are small (0.134 Mt in 2014) but increasing; in Gansu province, east of Qinghai, NOx emissions peaked at about 0.481 Mt in 2011 and decreased to 0.418 Mt in 2014.

Shangdianzi is a regional GAW site, located approximately

**Table 1**
Number of EU sites in each trend type category subset by EU AirBase classification. Values in parentheses indicate the percent of sites in each classification that fall into each category.

| Trend Type | RB[a] | RI[a] | SB[a] | SI[a] | ST[a] | UB[a] | UI[a] | UT[a] | Total |
|---|---|---|---|---|---|---|---|---|---|
| 0 (No Trend) | 11 (11%) | | 1 (2%) | | 1 (50%) | | | | 13 (5%) |
| 1a | 23 (23%) | 4 (80%) | 36 (55%) | 4 (44%) | | 36 (53%) | 2 (100%) | 13 (59%) | 118 (43%) |
| 1b | 34 (33%) | | 7 (11%) | 1 (11%) | | 5 (7%) | | 1 (5%) | 48 (17%) |
| 1c | 1 (1%) | | | | | | | | 1 (0.4%) |
| 2 | 12 (12%) | 1 (20%) | 12 (18%) | 2 (22%) | | 22 (32%) | | 7 (32%) | 56 (20%) |
| 3 | 12 (12%) | | 7 (11%) | | | 2 (3%) | | 1 (5%) | 22 (8%) |
| 4 | 5 (5%) | | | | | | | | 5 (2%) |
| X | 1 (1%) | | 2 (3%) | | | 1 (1%) | | | 4 (1%) |
| Incomplete | 3 (3%) | | 1 (1%) | 2 (22%) | 1 (50%) | 2 (3%) | | | 9 (3%) |
| Total | 102 | 5 | 66 | 9 | 2 | 68 | 2 | 22 | 276 |

[a] RB, rural background; RI, rural industrial; SB, suburban background; SI, suburban industrial; ST, suburban traffic; UB, urban background; UI, urban industrial; UT, urban traffic.

**Table 2**
Number of US sites in each trend type category from the scatter dataset (see Supplement Appendix D) by degree of urbanization. Values in parentheses indicate the percent of rural, suburban, or urban sites that fall into each category.

| Trend Type | Rural | Suburban | Urban | Total |
|---|---|---|---|---|
| 0 (No trend) | 5 (6%) | 0 (0%) | 0 (0%) | 5 (3%) |
| 1a | 31 (36%) | 44 (76%) | 44 (86%) | 119 (61%) |
| 1b | 26 (30%) | 11 (19%) | 5 (10%) | 42 (21%) |
| 1c | 4 (5%) | 0 (0%) | 0 (0%) | 4 (2%) |
| 2 | 4 (5%) | 1 (2%) | 2 (4%) | 7 (4%) |
| 3 | 7 (8%) | 1 (2%) | 0 (0%) | 8 (4%) |
| 4 | 9 (10%) | 1 (2%) | 0 (0%) | 10 (5%) |
| 7 | 1 (1%) | 0 (0%) | 0 (0%) | 1 (<1%) |
| Total | 87 | 58 | 51 | 196 |

**Table 3**
Sites in China used in the study.

| Site | Years in Study | Land Use[a] | Elevation (m) | Trend Type |
|---|---|---|---|---|
| **Mainland** | | | | |
| Mt. Waliguan | 2000–2015 | GB | 3810 | 7 |
| Shangdianzi | 2004–2015 | RB | 294 | 7 |
| Longfengshan | 2006–2015 | RB | 310 | X |
| **Hong Kong** | | | | |
| Central/Western | 1990–2015 | U | 16 | 8 |
| Kwai Chung | 1990–2015 | U | 13 | 8 |
| Tap Mun | 1998–2015 | R | 11 | X |
| Tai Po | 1998–2015 | S | 25 | 8 |
| Yuen Long | 1995–2015 | S | 25 | 8 |
| Hok Tsui | 1994–2015 | R | 60 | X |

[a] GB, global baseline; RB, regional background; U, urban; R, rural; S, suburban.

100 km northeast of the urban center of Beijing. The 30 km radius surrounding the site contains only small villages with a sparse population and insignificant anthropogenic sources. The observations of pollutants at Shangdianzi reflect the regional-scale air quality of North China (Lin et al., 2008; Xu et al., 2009a). However, the site is often impacted by pollution transported from the North China Plain (NCP), particularly in the summer (Lin et al., 2008; Ge et al., 2012). In the NCP, total NOx emissions have been large for many years; a maximum of 2.348 Mt was reached in 2011 that decreased to 1.946 Mt in 2014 (http://data.stats.gov.cn/).

Longfengshan is a regional background GAW site in Northeast China. It is located on top of a hill on the eastern edge of the Northeast China Plain, bordering on the Changbai Mountains (Xu et al., 1998). The site may be impacted by biomass burning emissions (i.e., biofuels and open burning after harvest). Previous studies (Xu et al., 1997, 2009b) suggest that air masses from the cities of Harbin (140 km northwest), Jilin (130 km southwest), and Changchun (200 km southwest) can arrive at Longfengshan, with those from the southwest sector causing enhanced concentrations of reactive gases at the site.

For the six Hong Kong sites, hourly average $O_3$ data were obtained from the Hong Kong Polytechnic University (HKPU) for the Hok Tsui station and the Hong Kong Environmental Protection Department (HKEPD) for the other stations (data available at http://www.aqhi.gov.hk). The Hok Tsui station (operated by the HKPU since 1994) was established to monitor changes in the composition of background air and to investigate the chemistry and transport of air pollution in subtropical Asia (Wang et al., 2009). Hok Tsui is upwind of Hong Kong's urban areas most of the time. Pollution-laden continental flow from the north, in conjunction with the stable and warm weather, contributes to the $O_3$ maximum in autumn (i.e., September, October, and November). The Tap Mun station is a rural air quality monitoring station on the Grass Island northeast of Hong Kong. The site is not affected by local residential and road traffic emissions but is influenced by transported anthropogenic emissions. Central Western and Kwai Chung are urban stations that are significantly influenced by local residential and traffic emissions. Tai Po and Yuen Long are located in suburban areas of the New Territory, which is adjacent to Shenzhen, a megacity in China. The two stations are influenced by local residential and traffic emissions and pollutions transported from mainland China.

### 2.2. Statistical tests

Analyses were conducted on a site-by-site basis. An important consideration in selecting statistical tests for assessing trends was the requirement that the same statistical methods be applied across all sites. The large amount of data to be characterized

precluded a detailed review of the data from every site to determine (1) an appropriate analytical functional form that fit the data and (2) whether a regression approach (e.g., linear or non-linear) would satisfy the assumptions associated with its use. Consequently, the nonparametric Mann-Kendall (M-K) test (Mann, 1945) and the Theil-Sen (T-S) estimator (Theil, 1950a, 1950b; 1950c; Sen, 1968) were selected because they require no assumptions regarding functional form or statistical distribution for the data and are resistant to outliers. In addition, these methods do not require consideration of whether trends are linear or non-linear. The T-S estimator was used to determine the magnitude and direction of the trend for a given time period (i.e., annual, monthly, hour of day); the M-K test was used to determine the significance of each trend using a significance threshold of $p < 0.05$. The software used to perform the statistical tests was R (R Development Core Team, 2008; R Core Team, 2016; Jassby and Cloern, 2016).

### 2.3. Characterizing distribution changes in hourly ozone

To characterize trends in hourly $O_3$ concentrations, $O_3$ values were grouped into 5 ppb bins for each site (i.e., $0 \leq O_3 < 5$, $5 \leq O_3 < 10$, $10 \leq O_3 < 15$, etc.) (Fig. 2a) and the number and percentage of hourly $O_3$ observations contained in each bin by year was tabulated. For all time periods with less than 75% data completeness, results were not presented. The M-K and T-S estimator described above were then used to determine the multi-year trends in the frequency of hourly $O_3$ concentrations falling into each bin.

The T-S estimator is the median of the slopes between all possible pairs of data points. Therefore, in cases where more than 70% of the data points are zero, the slope must by definition be zero since over half of the pairwise slopes are zero. However, because the M-K test is not based on the T-S estimator itself, but on determining the presence of a monotonically increasing or decreasing sequence, there were cases when a T-S slope of zero was associated with a significant trend. For example, in a time series of length 35 years, where the first 10 values are monotonically decreasing and the last 25 values are zero, the M-K test will result in a significant trend and the T-S slope will be zero. In the US data analyzed, this type of pattern occurred quite often for high $O_3$ concentration bins at the beginning of the time series. As emissions controls were implemented in the US, the frequency of the high $O_3$ values decreased and in many cases did not occur after the beginning of the time series. In these cases, the significant M-K result represents a real physical process, but the T-S estimator did not permit a determination of the magnitude and sign of the trend. To address this issue, a second step in the analysis was implemented only for cases in which the initial T-S slope estimate was zero. In those cases, a weighted moving average time-series was calculated from the original frequency values. The weighting function is the standard Normal density (i.e., a Normal density with a mean of 0 and a standard deviation of 1; see Supplemental Appendix E for details and an example of this calculation). The T-S slope was then calculated from the weighted moving average time series, and the value determined from the moving average replaced the original T-S slope. Regardless of which method was applied to determine the T-S slope estimate, the M-K test was conducted using the original time series.

The patterns of changes in hourly average $O_3$ concentration distributions were separated into ten distinct 'trend type' categories. The classification of sites into trend types provides a way to generalize how metrics respond to similar patterns of change across the $O_3$ distribution. For each site, we identify what portion of the distribution of hourly average concentrations has shifted. In the description of the trend type patterns, we discuss high, middle, and low $O_3$ concentrations, which do not refer to absolute concentrations but rather describe relative changes in the distribution at any particular site. For characterizing patterns of change for the distributions, the trend types (the algorithm procedures applied for identifying trend types are described in Supplement Appendix B) are described as follows:

- **Trend Type 0:** No trend.
- **Trend Type 1**: Both ends of the distribution shift toward the center. (Decreasing frequency of high and low concentrations).
- **Trend Type 2**: Low end shifts upward but high end does not change. (Decreasing frequency of low concentrations; increasing frequency of middle concentrations).
- **Trend Type 3**: High end shifts downwards but no change at lower end (Decreasing frequency of high concentrations; increasing frequency of middle concentrations).
- **Trend Type 4**: Entire distribution shifts downwards (Decreasing frequency of high concentrations, increasing frequency of low concentrations).
- **Trend Type 5**: The distribution shifts from the center toward both the high and the low ends of the distribution. (Increasing frequency of high and low concentrations).
- **Trend Type 6**: The middle of the distribution shifts downward but the high end does not change. (Increasing frequency of low concentrations, decreasing frequency of middle concentrations).
- **Trend Type 7**: The middle of the distribution shifts upward but the low end does not change. (Increasing frequency of high concentrations, decreasing frequency of middle concentrations).
- **Trend Type 8**: Entire distribution shifts upwards. (Increasing frequency of high concentrations, decreasing frequency of low concentrations).
- **Trend Type X**: Complex trends that do not fall into any of the categories listed above. It is not possible to categorize portions of the $O_3$ distribution into "low", "middle", and "high" for this trend type because the directions of the trends shift more than two times across the distribution (see Fig. 7 and Supplement Appendix A Figs. A.1 and A.2).

Because relative shifts of low and high hourly concentrations within the Trend Type 1 distribution can influence the median concentration, Trend Type 1 sites were further grouped into three subcategories based upon trends in the median concentration: (1) "1a" sites had increasing trends in the median; (2) "1b" sites had no trend in the median; and (3) "1c" sites had decreasing trends in the median.

### 2.4. Human health and vegetation exposure metrics

From those human health and vegetation metrics included in the Tropospheric Ozone Assessment Report (TOAR) research program (http://www.igacproject.org/sites/all/themes/bluemasters/images/TOAR_ListOf_Metrics.pdf), 14 were selected for analysis in this study. A full description of the calculation method for each exposure metric, including data capture criteria, is provided in Supplement Appendix C. We explored how each of the exposure metrics responded to changes over time at each of the sites analyzed. These 14 metrics were calculated for each year that met the data completeness requirement. These yearly values were used to construct a time series for each exposure metric and the T-S slope was calculated with significance based on the M-K test at the $p < 0.05$ level. Across all sites, the trend of each of the exposure metrics was compared to the trend type category that was determined using methods described in Section 2.3.

An additional data completeness protocol was implemented to guarantee that sufficient data were available over the entire time

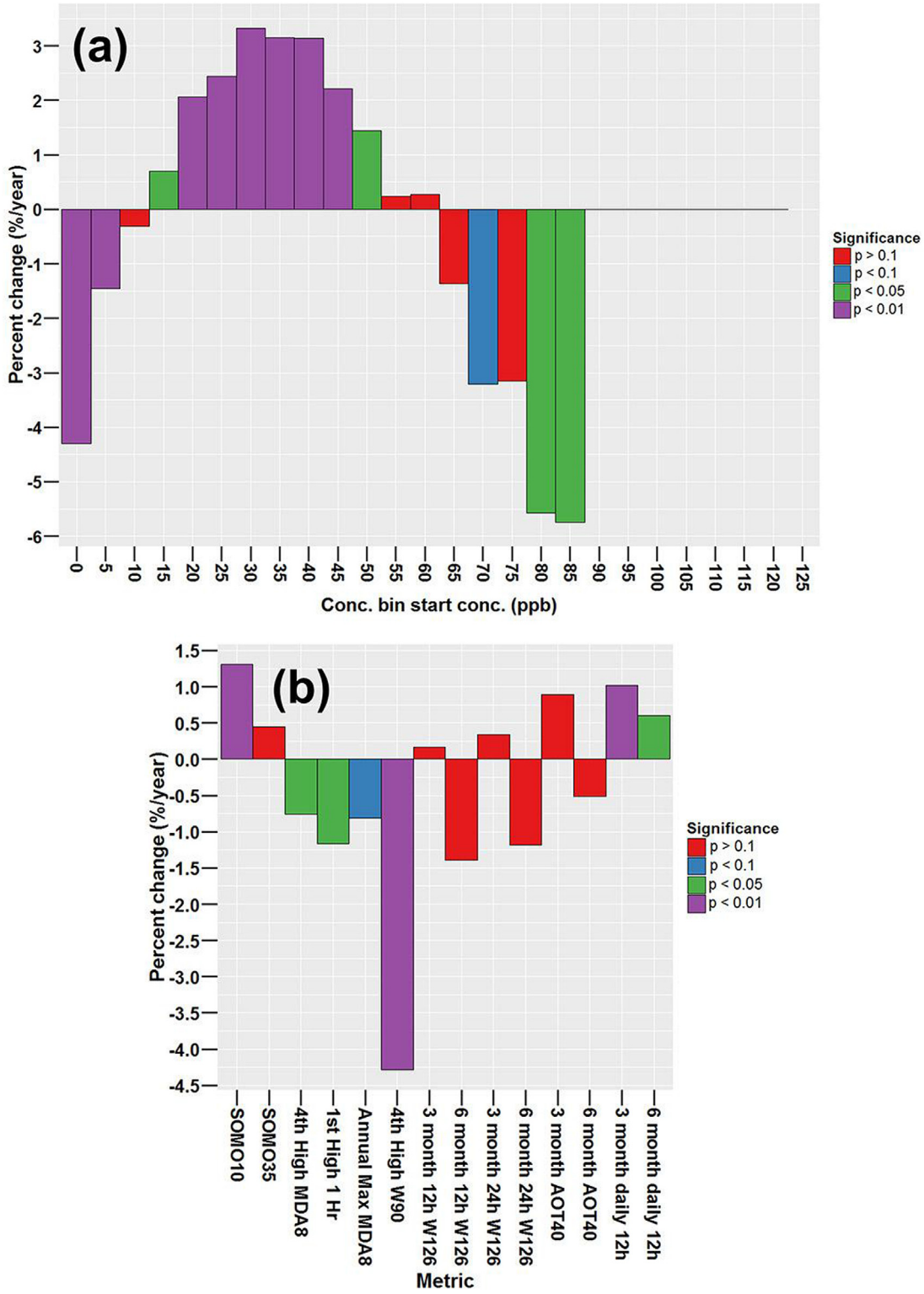


**Fig. 2.** Theil-Sen trend (%/year) (1990–2013) at Berlin, Germany (EU AirBase ID: DEBE034): for (a) $O_3$ concentrations in each bin and (b) 6 human health and 8 vegetation $O_3$ metrics. For this study, $p < 0.05$ is used to determine significance using the Mann-Kendall test. This site is Trend Type 1a.

series. For M-K and T-S slope estimates, the fraction of missing slopes associated with the first and last fifths of the data were calculated as described by Schertz et al. (1991) so that the appropriateness of slope estimates could be assessed and results flagged.

The change in the frequency of absolute hourly $O_3$ concentrations influences the change in the magnitude of an exposure metric. Therefore, we identify those metrics that are mostly influenced by different portions of the $O_3$ distribution, specifically the (1) high concentrations, (2) moderate and high concentrations, (3) moderate concentrations, and (4) all concentrations (i.e., low, moderate, and high). The 14 exposure metrics are grouped as follows:

#### 2.4.1. Exposure metrics influenced by high hourly average $O_3$ concentrations

- annual 4th highest daily max 8-h $O_3$ concentration (A4MDA8) based on the US EPA protocol used in the 2008 8-h standard (US EPA, 2014b) (human health).
- annual max daily 8-h $O_3$ concentration (AmaxMDA8) based on the US EPA protocol used in the 2008 8-h standard (US EPA, 2014b) (human health).
- annual max daily 1-h average concentration (AmaxMDA1) (US EPA, 2014b) (human health).
- 4th highest W90 (A4W90) (5-h accumulation as described in Lefohn et al., 2010a) (human health).

The A4MDA8 metric is used by the US EPA to assess attainment of the $O_3$ NAAQS over a 3-year period.

#### 2.4.2. Exposure metrics influenced by moderate and high concentrations

- SOMO35 (Daily maximum 8-h concentrations used to determine SOMO35 were calculated as described in European Council Directive, 2008/50/EC) (human health).
- 12-h W126 3-month (US EPA, 2014b) (vegetation).
- 12-h W126 6-month (US EPA, 2013) (vegetation).
- 24-h W126 3-month (US EPA, 2013) (vegetation).
- 24-h W126 6-month (US EPA, 2013) (vegetation).
- 12-h AOT40 3-month (European Council Directive, 2008/50/EC) (vegetation).
- 12-h AOT40 6-month (European Council Directive, 2008/50/EC) (vegetation).

The seven exposure metrics associated with moderate and high concentrations within a distribution all constitute cumulative exposure metrics calculated either as a sum or weighted sum across months.

#### 2.4.3. Exposure metrics primarily influenced by moderate concentrations

- Daily 12-h (0800–1959h) average averaged over 3-months (Avnery et al., 2011; Van Dingenen et al., 2009) (vegetation).
- Daily 12-h (0800–1959h) average averaged over 6-months (vegetation).

#### 2.4.4. Exposure metric influenced by the low, moderate, and high concentrations

- SOMO10 (Daily maximum 8-h concentrations used to determine SOMO10 were calculated as described in European Council Directive, 2008/50/EC) (human health).

While in this study we do not assign an absolute concentration range specific to the term "high," "moderate," and "low," we discuss in Section 4.3 how quantitative differences in absolute concentrations influence the statistical significance of changes that occurred in the exposure metrics across sites. For ease in summarizing the results of our analyses in the main part of our paper, we focused on the following 6 exposure metrics: (1) A4MDA8, (2) SOMO35, (3) 12-h AOT40 3-month, (4) 12-h W126 6-month, (5) daily 12-h (0 800–1959h) average averaged over 6-months, and (6) SOMO10, which demonstrate the range of behavior observed for the entire set of 14 metrics and cover metrics relevant for both human health (A4MDA8, SOMO35, SOMO10) and vegetation effects (AOT40, W126, daily 12-h). Across the 14 metrics, and even the subset of 6 metrics, there are similarities in the trend behavior of some of the exposure metrics as the hourly average concentrations change within distributions. Because the relevance for assessment and quantification of $O_3$ human health and vegetation impacts has been separately demonstrated for each of the metrics, we include analysis of the behavior pattern of the trends for all 14 effects metrics in Supplement Appendix A.

## 3. Results

The response of the 14 metrics over time is associated with which part of the hourly $O_3$ concentration distribution changes. Therefore, a change in the distribution of hourly $O_3$ at a specific site may be associated with different responses for different metrics. As a result, different conclusions may be reached concerning effects assessments and emission control strategies. In Section 3.1, we describe the patterns of shifting hourly average $O_3$ concentrations that have occurred at the EU, US, and Chinese sites and assign each specific pattern to a specific trend type category identified in Section 2.3. We then focus on the behavior of those metrics described in Section 2.4 influenced by shifts in the (1) high, (2) moderate and high, (3) moderate, and (4) low, moderate, and high concentration ranges to better understand the relationship between the metrics and the shifts that occur over time within the various parts of the distributions.

### 3.1. Changes in the distribution in hourly average concentrations

Tables 1 and 2 summarize the trend type assignments for the 276 EU and 196 US monitoring sites, respectively. Trend Type 1 (i.e., compression of the high- and low-end concentrations within the distribution, shifting more $O_3$ concentrations toward the center) was the most predominant trend pattern (60% of EU sites (167)) and 84% of US sites (165)). Figs. 2 and 3 illustrate the pattern of changing hourly average concentrations associated with Trend Type 1 for sites at Berlin, Germany (1990–2013) and Beltsville, MD USA (1989–2014), respectively. For both sites, the median (i.e., 50th percentile) concentrations increased and so they were characterized as Trend Type 1a (see Section 2.3). The majority of the EU and US Trend Type 1 sites were classified as Trend Type 1a (increasing median); almost 30% were classified as Trend Type 1b (no trend in the median). For the EU sites, a substantial number had only increasing low-end concentrations (i.e., Trend Type 2; 56 sites) or only decreasing high-end concentrations (i.e., Trend Type 3; 22 sites). The remaining 11% of sites were split between Trend Types 0, 1c, 4, X, and Incomplete. The 15% of US sites that were not Trend Type 1a or 1b were split between Trend Types 0, 1c, 2, 3, 4, and 7. Not all sites experienced significant changes in their distributional patterns. Thirteen sites in the EU and five sites in the US exhibited no trends (i.e., Trend Type 0).

Table 3 describes the land use characteristics and summarizes the trend types for the three sites in mainland China and six sites in

Hong Kong. Trends at the nine sites were different from the trends exhibited at EU and US sites, likely reflecting the substantially different emissions environment and also possibly being more influenced by inter-annual variability due to the shorter monitoring time periods at several of the sites. All nine of these sites were characterized as either Trend Types 7, 8 or X (i.e., complex trends that could not be categorized). At Mt. Waliguan (Fig. 4a), there was an absence of concentrations below 25 ppb between 2000 and 2015. The trend pattern showed a decreasing frequency of hourly average $O_3$ concentrations in the 35 and 45 ppb bins, with an increasing frequency in the 55 and 60 ppb bins. The trend type assigned to these patterns (2000–2015) was Trend Type 7 (i.e., the middle of the distribution shifts upward but the low end does not change). This assignment demonstrates a somewhat arbitrary distinction between Trend Type 2 and Trend Type 7 when a cutoff (35 ppb) is used to distinguish between the "low end" and middle of the distribution (Fig. 4a). A Trend Type 2 assignment could have resulted if a lower cutoff concentration were used. At the Shangdianzi site (2004–2015), the middle of the distribution shifted upward but the low end did not change (Fig. 5a). The algorithm described in Supplement Appendix B resulted in Trend Type 7 assignment, but decreasing trends in the frequency of concentrations between 20 and 35 ppb share some of the characteristics of a Trend Type 8 site. The assignment of this site to Trend Type 7 rather than to Trend Type 8 relied on the decision to classify decreases in the frequency of the 20–35 ppb concentrations as changes in moderate (for Trend Type 7), rather than low (Trend Type 8) concentrations. At the Longfengshan site, the mid-range concentrations shifted downward, resulting in an increasing frequency of low concentrations. However, there was one high concentration bin (115–120 ppb), which exhibited a decreasing trend (Fig. A.1). This site was characterized as Trend Type X.

For the six Hong Kong sites, four of the sites (i.e., Central Western, Kwai Chung, Tai Po, and Yuen Long) were characterized as Trend Type 8 (entire distribution shifts upwards), as illustrated in Fig. 6a for the Central Western site. The Hok Tsui and Tap Mun sites exhibited a complex trend type because of both increasing and decreasing trends in moderate $O_3$ concentration bins (Fig. 7a and Fig. A.2a, respectively).

### 3.2. Trends in exposure metrics and the relationship to trend type categories

The trend type distribution shifts described in Section 3.1 affect the trends of the human health and vegetation exposure metrics identified in Section 2.4. For example, Fig. 3 illustrates the relationship between changes in $O_3$ concentration distribution and the 6 human health and 8 vegetation exposure metrics at a site at Beltsville, Maryland between 1989 and 2014 (classified as Trend Type 1a). A second example of changes in the $O_3$ concentration distribution and the response of human health metrics is shown in Fig. 2 for a site in Berlin, Germany. Both Figs. 2 and 3 illustrate the phenomenon that metrics defined to assess the same $O_3$ impact (i.e., human health or vegetation), under the same changing patterns of $O_3$ concentrations, can exhibit differing, and opposing changes in their magnitude. For example, at the Berlin site, between 1990 and 2013, the magnitude of the human health metrics could be concluded to have decreased, not changed, or increased depending on the specific metric used to quantify the effect. Sections 3.2.1–3.2.4 describe general patterns in the relationship between $O_3$ distribution trend types across all the sites analyzed and trends for the 14 exposure metrics.

#### 3.2.1. Exposure metrics associated with high concentrations

The majority of sites analyzed in the EU and US experienced reductions in the high-end of the $O_3$ distributions (Trend Types 1, 3, and 4), and therefore decreasing trends in the magnitude of the four exposure metrics (A4MDA8, AmaxMDA8, AmaxMDA1, and A4W90) were mostly impacted by the changes in these higher concentrations (Tables 4 and 5, Table A.1 and A.2). There were no sites in the US and only 2 sites in the EU that experienced increasing trends in any of these metrics. At both EU and US sites, Trend Types 1a, 1b, 1c, 3, and 4 were most often associated with decreasing trends in these metrics, while Trend Types 0, 2, and 7 were more likely to be associated with no trend and in rare cases, increasing trends. Within each category, the EU sites experienced substantially fewer occurrences of significant trends than the US sites (Tables 4 and 5, Table A.1 and A.2). The reasons for this observation are discussed in Section 4.

In contrast, the A4MDA8, AmaxMDA8, AmaxMDA1, and A4W90 metrics either increased or had no trends at the Chinese sites (Table 6 and Table A.3). For Mt. Waliguan (Trend Type 7) and Longfengshan, there were no trends in these four exposure metrics (Fig. 4b and Fig. A.1b, respectively). For the site at Shangdianzi, the Trend Type 8 changes (i.e., entire distribution shifts upwards) resulted in increasing trends in the A4MDA8, AmaxMDA8, and A4W90 exposure metrics, but no trend in AmaxMDA1 (Fig. 5b). At five of the Hong Kong sites, all four exposure metrics increased (e.g., Figs. 6b and 7b); there were no trends calculated in any of these metrics at the Tap Mun Trend Type X site (Fig. A.2b).

#### 3.2.2. Exposure metrics associated with moderate and high concentrations

The seven metrics (SOMO35, 3-month 12-h W126, 6-month 12-h W126, 3-month 24-h W126, 6-monthy 24-h W126, 3-month 12-h AOT40, and 6-month 12-h AOT40) either decreased or had no trend at most EU and US sites analyzed, although some metrics increased at a small number of sites in both regions. Decreasing trends occurred more for the 6-month compared to the 3-month vegetation metrics. The 3-month season (defined to be representative of the wheat growing season in different climate zones) specifications are detailed in http://www.igacproject.org/sites/all/themes/bluemasters/images/TOAR_ListOf_Metrics.pdf. In many regions in the EU and US, this season occurs earlier in the year when regional photochemical $O_3$ production makes a smaller relative contribution to $O_3$ concentrations, and therefore is less likely to decrease in response to local or regional NOx emissions reductions compared to the fixed 6-month season (April–September). Sites with Trend Types 1b, 1c, 3, and 4 were more likely to have decreasing trends in these seven metrics than Trend Type 1a and 2 sites. In the US, these trend types (i.e., 1b, 1c, 3, and 4) had predominantly decreasing trends with a smaller number of sites experiencing no trend, while in the EU, no trend was most common for sites with these trend types. Most Trend Type 1a sites in the EU had no trend for these metrics, while in the US Trend Type 1a sites were predominantly decreasing for some metrics and had no trends for others. Similar to the metrics focused on the higher concentrations (Section 3.2.1), there were fewer significant trends in these metrics across the EU sites analyzed than the US sites (Tables 4 and 5, and Table A.4-A.9).

The results at the 9 Chinese sites for these metrics were varied (Table 6 and Table A.10-A.12). For the Mt. Waliguan site, only the SOMO35 exposure metric increased with no trend for other metrics (Fig. 4b). The increase in the SOMO35 metric appears to be caused by increases in the middle of the distribution because no significant trends occurred above 70 ppb. In contrast, at the Shangdianzi site (Trend Type 7), all seven of the exposure metrics increased (Fig. 5b). At Longfengshan, the 3-month 12-h W126, 24-h W126, and AOT40 metrics exhibited decreasing trends (Fig. A.1b), while the other four metrics experienced no trend. The 3-month accumulation period for this site was March–May. The month of April experienced

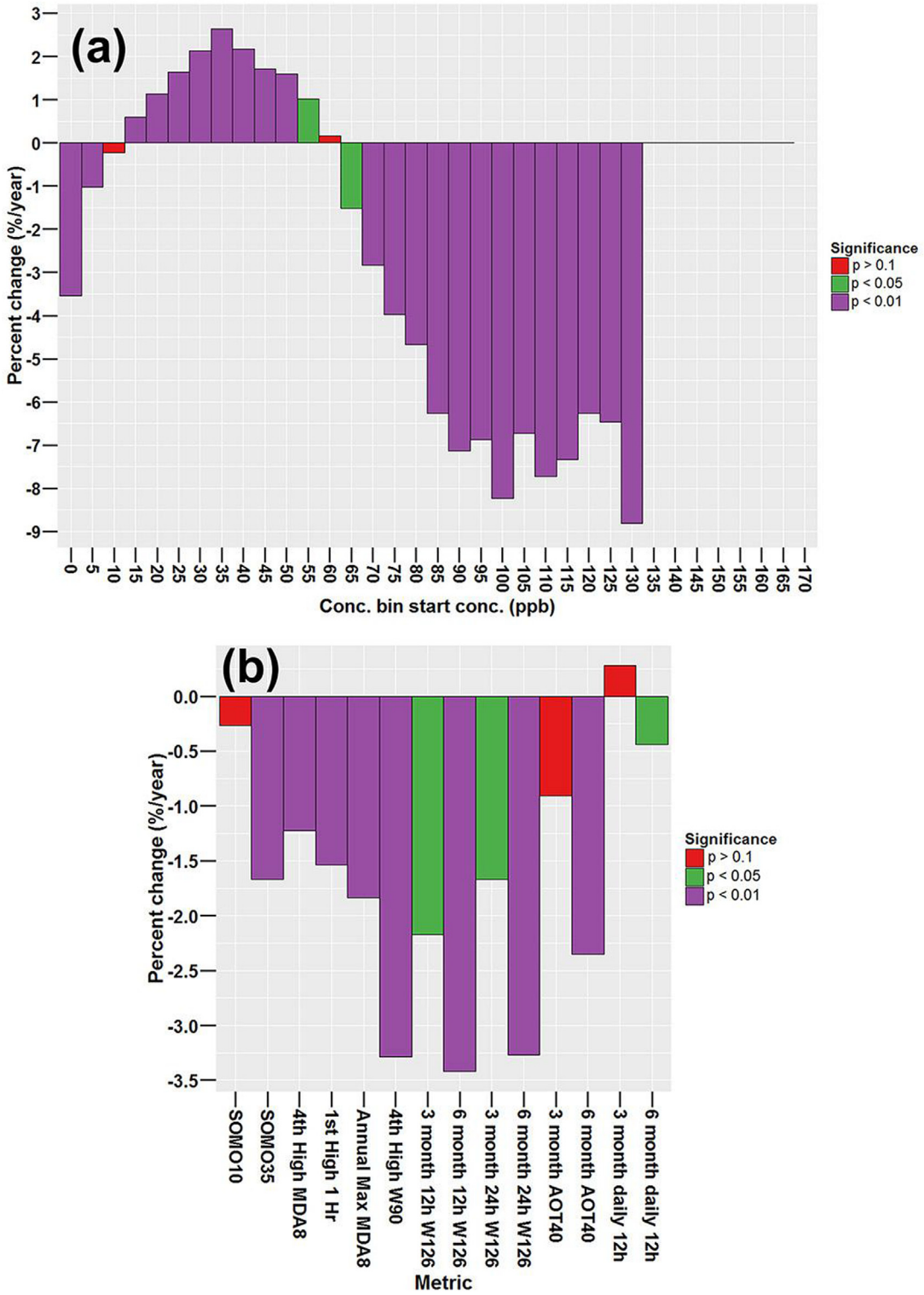


**Fig. 3.** Theil-Sen trend (%/year) (1989–2014) at Beltsville, Maryland (EPA AQS ID: 240339991-1) for (a) $O_3$ concentrations in each bin and (b) 6 human health and 8 vegetation $O_3$ metrics. For this study, $p < 0.05$ is used to determine significance using the Mann-Kendall test. This site is Trend Type 1a.

decreasing trends in the mid-concentrations with shifts downward into the lower values; this may be associated with the decreasing trends for the 3-month metrics. At four of the Hong Kong sites (Central Western, Hok Tsui, Kwai Chung, and Yuen Long), all seven exposure metrics increased (Table 6 and Table A.10-A.12). The Tai Po site experienced increasing trends in the SOMO35, 6-month 12-hW126, 6-month 24-h W126, 3- and 6-month AOT40 metrics, but no trend for the 3-month 12-h W126 and 3-month 24-h W126 metrics. No significant trends were calculated for any of the seven metrics at Tap Mun (Fig. A.2b).

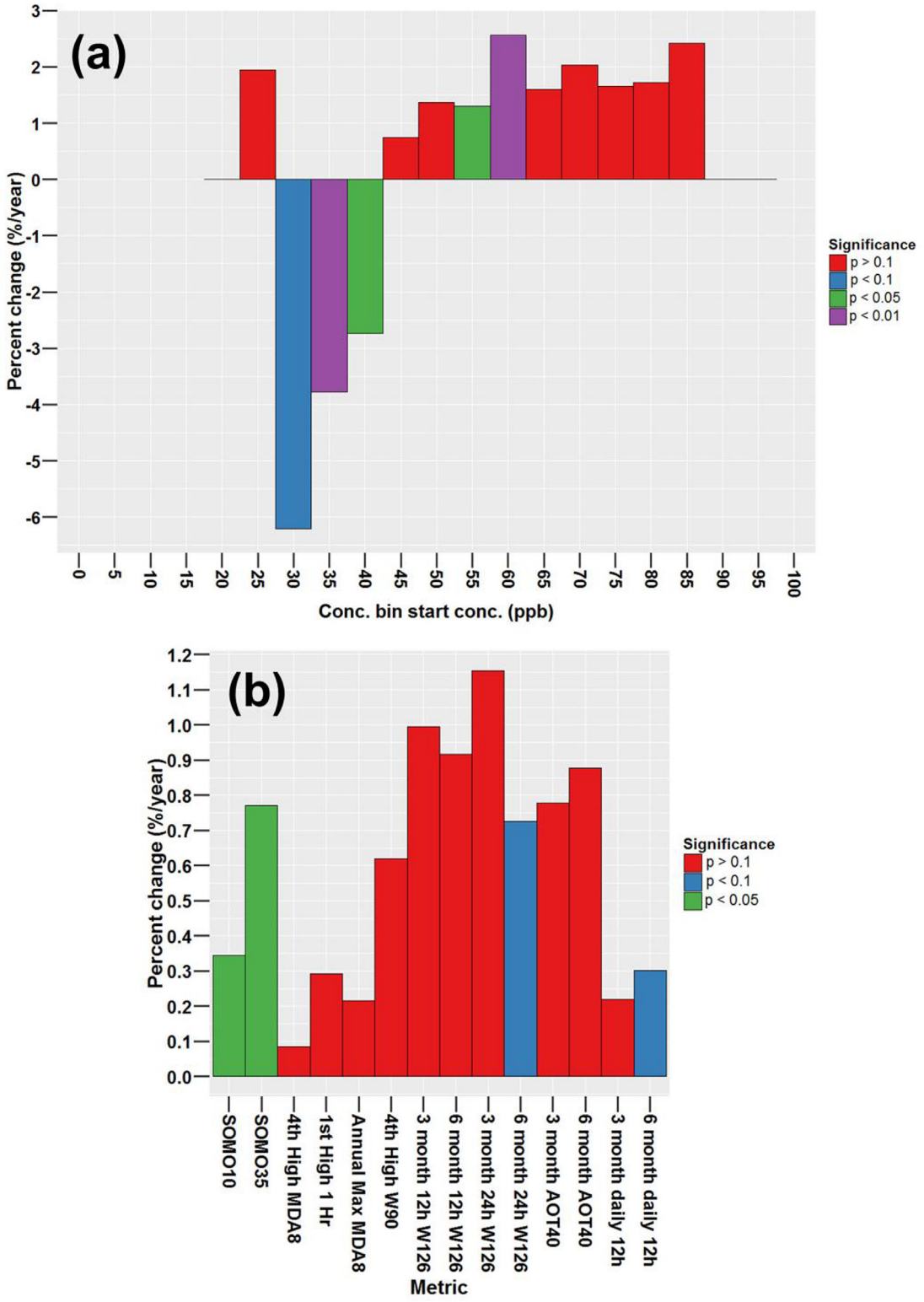


**Fig. 4.** Theil-Sen trend (%/year) (2000–2015) at Mt. Waliguan, China for (a) $O_3$ concentrations in each bin and (b) 6 human health and 8 vegetation $O_3$ metrics. For this study, $p < 0.05$ is used to determine significance using the Mann-Kendall test. The site is Trend Type 7.

*3.2.3. Exposure metrics associated primarily with moderate concentrations*

The 6-month and 3-month 12-h (0800–1959h) average exposure metrics did not show significant trends at most EU and US sites with Trend Types 1a, 1b, 2, and 3 (Tables 4 and 5, Table A.8 and A.9). For the EU sites analyzed, there were more increasing than decreasing trends, although there was no trend at the majority of sites for both metrics (Table 4 and Table A.8). For the US sites, there were more decreasing than increasing trends for the 6-month 12-h metric; for the 3-month 12-h metric, there were more sites with

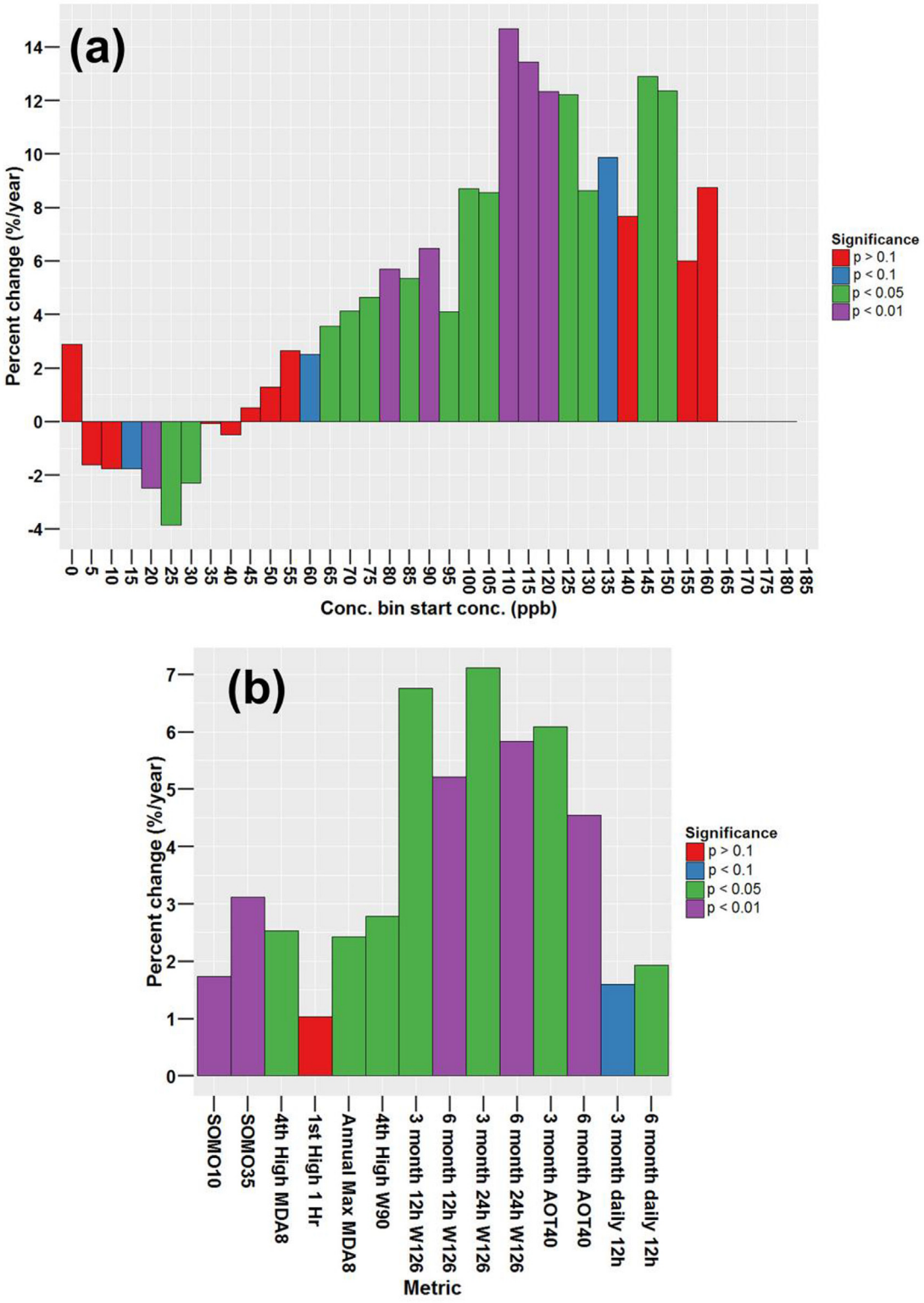


**Fig. 5.** Theil-Sen trend (%/year) (2004–2015) at Shangdianzi, China for (a) $O_3$ concentrations in each bin and (b) 6 human health and 8 vegetation $O_3$ metrics. For this study, $p < 0.05$ is used to determine significance using the Mann-Kendall test. The site is Trend Type 7.

increasing than decreasing trends. There were a substantial number of sites with no trend for both metrics (Table 5 and Table A.9). The tendency for the 3-month 12-h metric to increase at more sites than the 6-month 12-h metric may be associated with the fact that many of the 3-month averaging periods included mainly spring months. During the summer months, there are more decreasing high $O_3$ concentrations compared to spring months that possibly could influence the decreasing trends identified in the 6-month 12-h metric.

The two 12-h metrics are associated with the mid-range

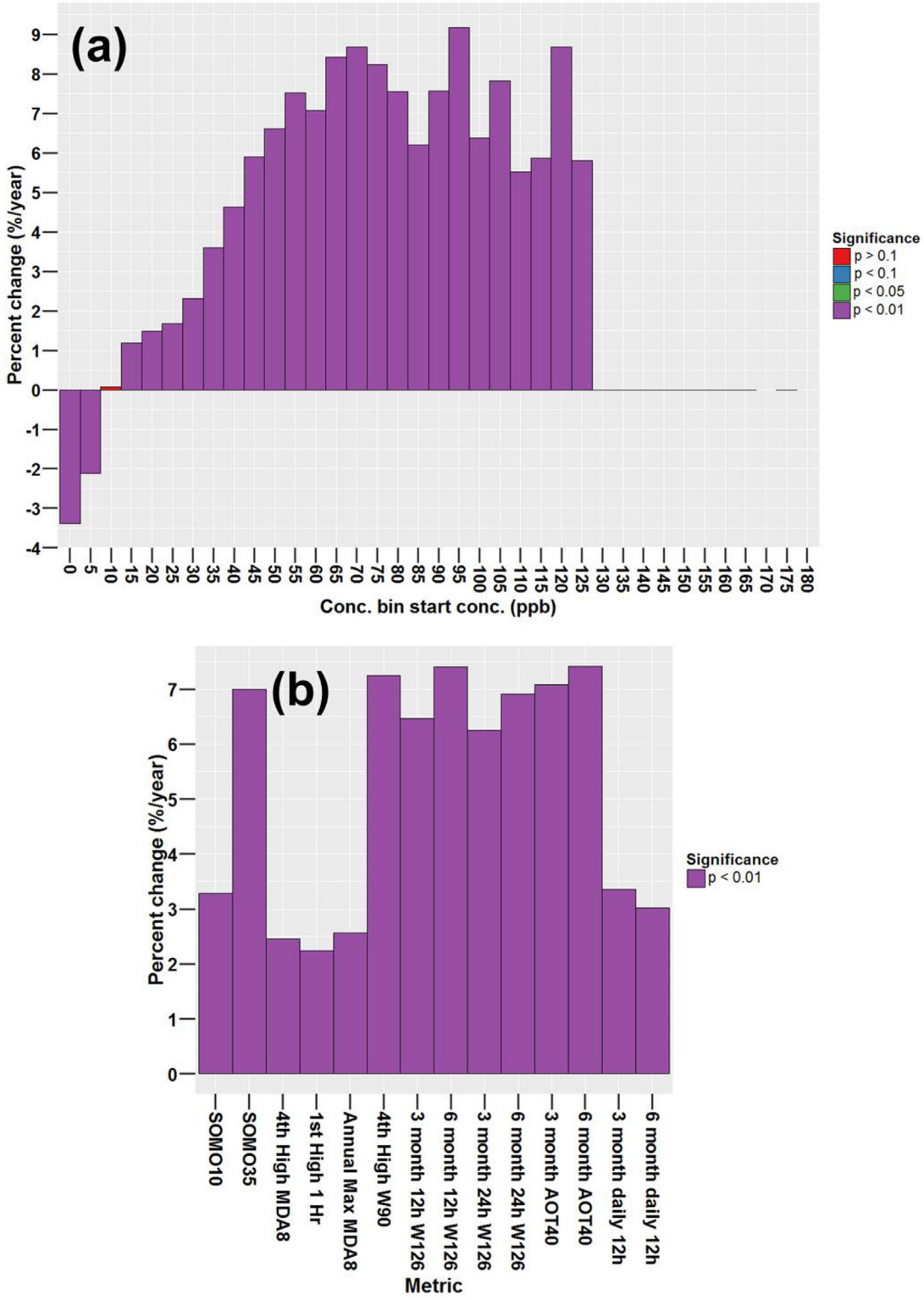


**Fig. 6.** Theil-Sen trend (%/year) (1990–2015) at Central Western, Hong Kong, China for (a) $O_3$ concentrations in each bin and (b) 6 human health and 8 vegetation $O_3$ metrics. For this study, $p < 0.05$ is used to determine significance using the Mann-Kendall test. The site is Trend Type 8.

concentrations within the hourly average concentration distribution. These metrics are equally impacted by all daytime values. Therefore, the increases in the more frequent low $O_3$ concentrations have a proportionally larger impact on these metrics than other metrics associated with vegetation effects. Hence, the 3-month 12-h mean metric had increasing trends at more sites than any other metric. Sites classified as Trend Types 1a and 2 were most likely to have increasing trends in the 12-h metrics at the EU and US sites (Tables 4 and 5, Table A.8 and A.9). The increasing annual median concentration for Trend Type 1a sites was generally

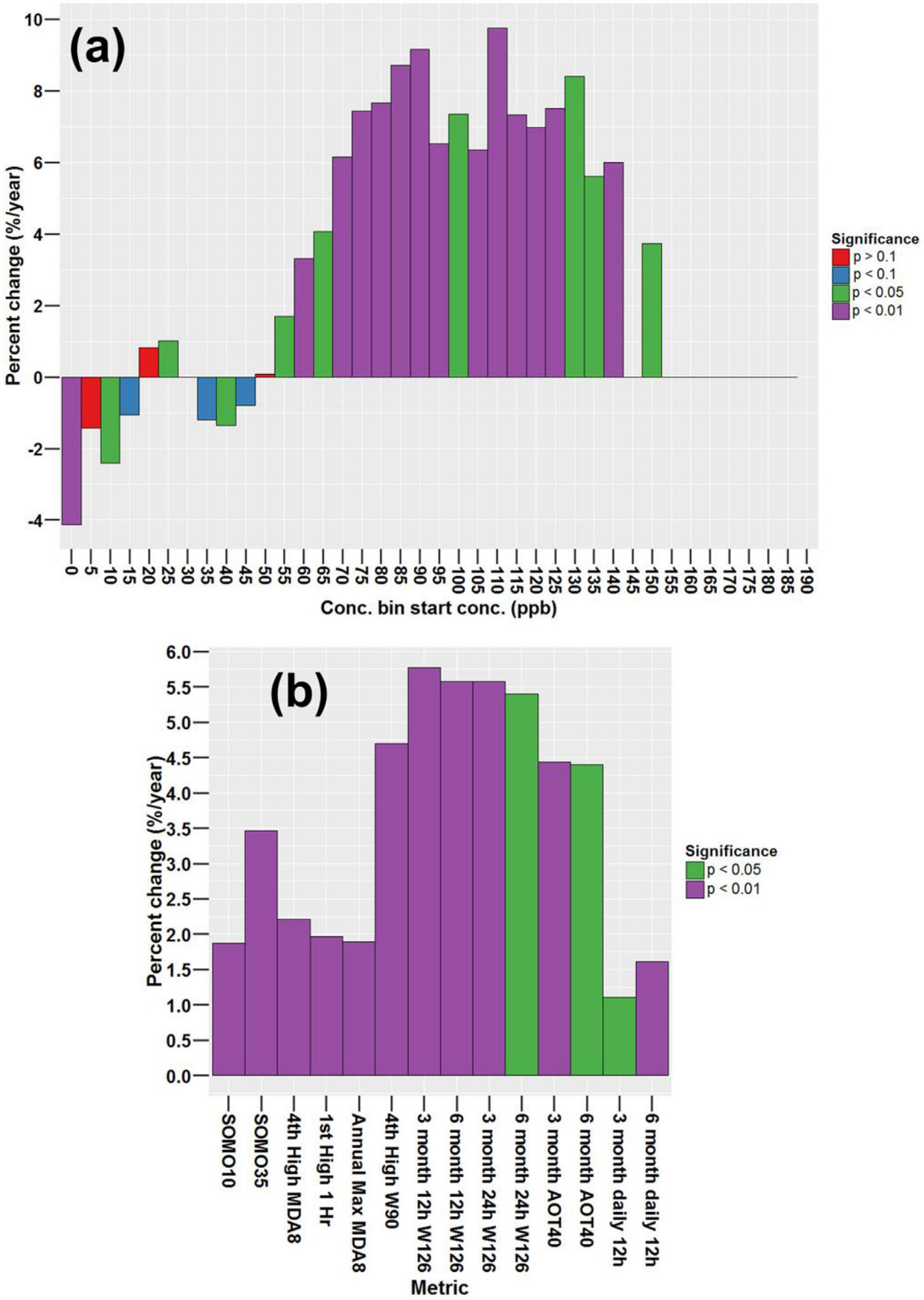


**Fig. 7.** Theil-Sen trend (%/year) (1994–2015) at Hok Tsui, Hong Kong, China for (a) $O_3$ concentrations in each bin and (b) 6 human health and 8 vegetation $O_3$ metrics. For this study, $p < 0.05$ is used to determine significance using the Mann-Kendall test. Trend type at this site was characterized as not matching the algorithms described in Supplement Appendix B (Trend Type X).

associated with increasing trends calculated in the 12-h metrics. However, even among the Trend Type 1a sites, where there is a compression of both ends of the distribution and the annual median concentration increases, more sites had no trends than increasing trends for these metrics (Tables 4 and 5, Table A.8 and A.9). As anticipated, for Trend Type 2 sites (shifting of the concentrations upwards), increasing trends occurred in the two 12-h metrics at many sites.

**Table 4**
Number of EU sites in each trend type category which had decreasing (Dec), no significant trend (NT), increasing (Inc), or incomplete (NA) trends in six $O_3$ metrics (A4MDA8, SOMO35, 3-month AOT40, 6-month 12-h W126, 6-month 12-h average, and SOMO10).

| | A4MDA8 | | | | SOMO35 | | | | 3-mon. AOT40 | | | | 6-mon. 12-h W126 | | | | 6-mon. 12-h avg. | | | | SOMO10 | | | |
|---|---|---|---|---|---|---|---|---|---|---|---|---|---|---|---|---|---|---|---|---|---|---|---|---|
| Trend Type | Dec | NT | Inc | NA | Dec | NT | Inc | NA | Dec | NT | Inc | NA | Dec | NT | Inc | NA | Dec | NT | Inc | NA | Dec | NT | Inc | NA |
| 0 (No trend) | 0 | 12 | 0 | 1 | 0 | 12 | 0 | 1 | 0 | 13 | 0 | 0 | 2 | 11 | 0 | 0 | 0 | 13 | 0 | 0 | 0 | 12 | 0 | 1 |
| 1a | 59 | 57 | 0 | 2 | 18 | 96 | 2 | 2 | 4 | 110 | 3 | 1 | 44 | 73 | 0 | 1 | 2 | 82 | 34 | 0 | 1 | 72 | 43 | 2 |
| 1b | 31 | 17 | 0 | 0 | 19 | 29 | 0 | 0 | 5 | 43 | 0 | 0 | 30 | 18 | 0 | 0 | 11 | 36 | 1 | 0 | 6 | 42 | 0 | 0 |
| 1c | 1 | 0 | 0 | 0 | 1 | 0 | 0 | 0 | 1 | 0 | 0 | 0 | 1 | 0 | 0 | 0 | 1 | 0 | 0 | 0 | 1 | 0 | 0 | 0 |
| 2 | 0 | 52 | 2 | 2 | 0 | 44 | 10 | 2 | 0 | 42 | 12 | 2 | 0 | 51 | 5 | 0 | 0 | 28 | 28 | 0 | 0 | 29 | 25 | 2 |
| 3 | 7 | 14 | 0 | 1 | 9 | 12 | 0 | 1 | 3 | 17 | 0 | 2 | 12 | 10 | 0 | 0 | 7 | 15 | 0 | 0 | 4 | 17 | 0 | 1 |
| 4 | 5 | 0 | 0 | 0 | 4 | 1 | 0 | 0 | 4 | 1 | 0 | 0 | 5 | 0 | 0 | 0 | 4 | 1 | 0 | 0 | 4 | 1 | 0 | 0 |
| Total | 103 | 152 | 2 | 6 | 51 | 194 | 12 | 6 | 17 | 226 | 15 | 5 | 94 | 163 | 5 | 1 | 25 | 175 | 63 | 0 | 16 | 173 | 68 | 6 |

**Table 5**
Number of US sites in each trend type category which had decreasing (Dec), no significant trend (NT), increasing (Inc), or incomplete (NA) trends in six $O_3$ metrics (A4MDA8, SOMO35, 3-month AOT40, 6-month 12-h W126, 6-month 12-h average, and SOMO10).

| | A4MDA8 | | | | SOMO35 | | | | 3-mon.AOT40 | | | | 6-mon.12-h W126 | | | | 6-mon. 12-h avg. | | | | SOMO10 | | | |
|---|---|---|---|---|---|---|---|---|---|---|---|---|---|---|---|---|---|---|---|---|---|---|---|---|
| Trend Type | Dec | NT | Inc | NA | Dec | NT | Inc | NA | Dec | NT | Inc | NA | Dec | NT | Inc | NA | Dec | NT | Inc | NA | Dec | NT | Inc | NA |
| 0 (No trend) | 0 | 5 | 0 | 0 | 0 | 5 | 0 | 0 | 0 | 5 | 0 | 0 | 0 | 5 | 0 | 0 | 0 | 5 | 0 | 0 | 0 | 5 | 0 | 0 |
| 1a | 99 | 19 | 0 | 1 | 53 | 56 | 9 | 1 | 30 | 70 | 18 | 1 | 88 | 25 | 4 | 2 | 40 | 64 | 15 | 0 | 34 | 62 | 22 | 1 |
| 1b | 41 | 1 | 0 | 0 | 38 | 4 | 0 | 0 | 27 | 14 | 0 | 1 | 40 | 2 | 0 | 0 | 33 | 9 | 0 | 0 | 32 | 10 | 0 | 0 |
| 1c | 3 | 0 | 0 | 1 | 3 | 0 | 0 | 1 | 4 | 0 | 0 | 0 | 3 | 0 | 0 | 1 | 4 | 0 | 0 | 0 | 3 | 0 | 0 | 1 |
| 2 | 1 | 6 | 0 | 0 | 0 | 4 | 3 | 0 | 0 | 2 | 5 | 0 | 0 | 5 | 2 | 0 | 0 | 3 | 4 | 0 | 0 | 4 | 3 | 0 |
| 3 | 8 | 0 | 0 | 0 | 7 | 1 | 0 | 0 | 4 | 4 | 0 | 0 | 7 | 1 | 0 | 0 | 6 | 2 | 0 | 0 | 7 | 1 | 0 | 0 |
| 4 | 10 | 0 | 0 | 0 | 10 | 0 | 0 | 0 | 9 | 1 | 0 | 0 | 10 | 0 | 0 | 0 | 9 | 1 | 0 | 0 | 10 | 0 | 0 | 0 |
| 7 | 0 | 1 | 0 | 0 | 0 | 1 | 0 | 0 | 0 | 0 | 1 | 0 | 0 | 1 | 0 | 0 | 0 | 1 | 0 | 0 | 0 | 1 | 0 | 0 |
| Total | 162 | 32 | 0 | 2 | 111 | 71 | 12 | 2 | 74 | 96 | 24 | 2 | 148 | 39 | 6 | 3 | 92 | 85 | 19 | 0 | 86 | 83 | 25 | 2 |

**Table 6**
Sites in mainland China and Hong Kong, China exhibiting decreasing (Dec), no significant trend (NT), increasing (Inc), or incomplete (NA) trend in six $O_3$ metrics (A4MDA8, SOMO35, 3-month AOT40, 6-month 12-h W126, 6-month 12-h average, and SOMO10).

| Site (Trend Type) | A4MDA8 | SOMO35 | 3-mon. AOT40 | 6-mon. 12-h W126 | 6-mon. 12-h avg. | SOMO10 |
|---|---|---|---|---|---|---|
| **Mainland** | | | | | | |
| Mt. Waliguan (7) | NT | Inc | NT | NT | NT | Inc |
| Shangdianzi (7) | Inc | Inc | Inc | Inc | Inc | Inc |
| Longfengshan (X) | NT | NT | Dec | NT | NT | NT |
| **Hong Kong** | | | | | | |
| Central/Western (8) | Inc | Inc | Inc | Inc | Inc | Inc |
| Kwai Chung (8) | Inc | Inc | Inc | Inc | Inc | Inc |
| Tap Mun (X) | NT | Inc | NT | NT | NT | Inc |
| Tai Po (8) | Inc | Inc | Inc | Inc | NT | Inc |
| Yuen Long (8) | Inc | Inc | Inc | Inc | Inc | Inc |
| Hok Tsui (X) | Inc | Inc | Inc | Inc | Inc | Inc |

Trends in the 12-h metrics varied among the Chinese sites. For Mt. Waliguan, there was no trend in either metric (Fig. 4b). In contrast, the 6-month 12-h metric (but not the 3-month metric) increased at Shangdianzi (Fig. 5b) for which the distribution shifted upwards and the median concentrations increased. For Longfengshan, the 3-month 12-h metric decreased and there was no trend in the 6-month 12-h metric (Fig. A.1b). For four of the Hong Kong sites (Central Western, Hok Tsui, Kwai Chung, and Yuen Long), the 3- and 6-month 12-h average metrics increased (Table 6 and Table A.12). The 6-month daily 12-h average metric increased at Tai Po, but not the 3-month daily average 12-h metric. No significant trends were identified for either 12-h metrics at Tap Mun.

### *3.2.4. Exposure metric associated with low, moderate, and high concentrations*

For the EU sites, there were more sites with increasing trends than sites with decreasing trends across all trend types for the SOMO10 metric although most sites had no trend (Table 4). Although substantial emissions reductions have occurred across Europe, decreasing trends in the SOMO10 metric were infrequent. Increasing trends were most common at Trend Type 1a and 2 EU sites compared to other trend type sites. In the US, sites with Trend Types 1b, 1c, 3, and 4 were more likely to experience decreasing trends in SOMO10, although 29% of US Trend Type 1a sites also had decreasing SOMO10 values (Table 5). For the US sites, the shifts from the lower concentrations to the middle of the distribution appeared to play less of a role than the reduction in the higher concentrations in influencing decreasing trends in SOMO10. This is in contrast to the EU sites, where the relative magnitude of the opposing shifts from (1) low concentrations to moderate concentrations and (2) high concentrations to moderate concentrations resulted more frequently in increasing SOMO10 values.

The SOMO10 exposure metric either increased or had no trend at the Chinese sites. The increasing trend in SOMO10 at Mt. Waliguan may be associated with the upward shift in moderate concentrations (i.e., 30, 35, 40, 55, and 60 ppb bins) because no significant trends occurred in the hourly concentrations above 70 ppb (Fig. 4b). At Shangdianzi, SOMO10 increased consistently

with the upwards shift across the concentration distribution (Fig. 5b). For Longfengshan, the SOMO10 metric had no trend (Fig. A.1b). The SOMO10 metric increased for all six Hong Kong sites.

## 4. Discussion and conclusion

### 4.1. Reasons associated with the predominant pattern of decreasing higher concentrations and increasing lower concentrations (Trend Type 1)

Low $O_3$ concentrations increasing toward moderate levels, while the high concentrations decreased (i.e., Trend Type 1) was the most common pattern identified at the EU and US sites. Decreases in the frequency and magnitude of high $O_3$ episodes in the EU and US have been reported in the literature (Butler et al., 2011; Cooper et al., 2010, 2012; Hogrefe et al., 2011; Koumoutsaris and Bey, 2012; Lefohn et al., 2010b; Sather and Cavender, 2012; Simon et al., 2015; Sicard et al., 2016). In addition, while many investigators have reported that low-end $O_3$ concentrations have increased in both regions (Chan, 2009; Chan and Vet., 2010; Cooper et al., 2010, 2012; Hogrefe et al., 2011; Koumoutsaris and Bey, 2012; Lefohn et al., 2010b; Torseth et al., 2012; Simon et al., 2015; Sicard et al., 2016; Wilson et al., 2012), some have reported no changes at some sites (Vautard et al., 2006; Cooper et al., 2012; Wilson et al., 2012; Simon et al., 2015).

Based on the scientific understanding of $O_3$ processes described in the Introduction, there are three main drivers that could contribute to the compression of the $O_3$ distribution: (1) changes in local and regional anthropogenic precursor emissions (NOx and VOC), (2) changes in $O_3$ contribution from long-range transport, and (3) changes in $O_3$ due to trends in climate-driven natural emissions and meteorology. While all three factors may contribute to some degree to the shifting $O_3$ distributions, both the increases in low $O_3$ and decreases in high $O_3$ concentrations are consistent with what would be expected from substantial regional NOx reductions as has been documented previously. Specifically, modeling studies have linked decreases in regional emissions to decreases in high $O_3$ episodes in the US (Tagaris et al., 2007; Gilliland et al., 2008; Fiore et al., 2009; Xing et al., 2015) and EU (Jonson et al., 2006; Vautard et al., 2006), as well as increases in low $O_3$ concentrations at the same locations where high concentrations decrease (Jonson et al., 2006; Hogrefe et al., 2011; Simon et al., 2013, 2016; Downey et al., 2015). Additional evidence that regional emissions reductions can increase low $O_3$ concentrations comes from studies of measured concentrations. For example, Simon et al. (2015) reported that over a period of large US NOx emissions reductions, increasing low $O_3$ concentrations occurred to a greater extent at more urbanized sites, indicating that reduction in local NOx scavenging was increasing these low $O_3$ concentrations beyond any increases that occurred in regional background. Jenkin (2008) reported that in the UK, increases in low-end $O_3$ concentrations occurred to a greater extent at inland urban and rural locations than at an upwind coastal location, concluding that increasing low-end $O_3$ was at least partly due to regional chemistry changes from emissions reductions rather than increases in global or regional background. In addition, both Simon et al. (2015) and Sicard et al. (2016) reported more ambient increases in low $O_3$ concentrations during winter, the time of year where NOx scavenging is most likely to be favored, than during summer when OPE will be high. Below, we discuss the evidence that long-range transport and climate change could also play a role in the prevalence of sites exhibiting a compression of the $O_3$ distribution.

In many parts of Asia, $O_3$ precursor emissions have increased substantially (Monks et al., 2015). Observational and modeling studies have demonstrated that $O_3$ can be transported long distances across the Pacific and Atlantic oceans and can influence ground-level $O_3$ concentrations in the EU and US (Stohl and Trickl, 1999; Li et al., 2002; Jaffe et al., 2003; Derwent, 2008; TF HTAP, 2010; Lin et al., 2012; Langford et al., 2015; Derwent et al., 2015). Additionally, observational studies have reported $O_3$ concentration increases in the free troposphere over the US since the mid-1990s, although that increase appears to have slowed recently (Cooper et al., 2010, 2012; Lin et al., 2015). The increase in free tropospheric $O_3$ is attributed to long-range transport from Asia and to the extent that it mixes down to the surface it could impact ground-level concentrations. Monks et al. (2015) also reported that globally free tropospheric $O_3$ is either increasing or remaining constant depending on the location, which also supports the possibility that long-range transport could contribute to increasing ground-level $O_3$ concentrations in some locations. Based on global modeling simulations, Lin et al. (2012) showed $O_3$ originating from Asian emissions could periodically contribute over 5 ppb (May–June) to ground-level MDA8 $O_3$ concentrations at certain locations in the Western US, but those contributions dropped off precipitously east of the Rocky Mountains. Thus, while Asian emissions have increased substantially over the time period of our study, their impacts on $O_3$ trends is anticipated to be limited mostly to the Western US, with reduced impact on the Eastern US. While previous work suggests long-range transport is most likely to cause enhanced $O_3$ concentrations at high elevations in the US Intermountain West (Lin et al., 2012), we observed no trends (i.e., Trend Type 0) at five sites in this region (e.g., Grand Canyon National Park, Arizona, 2073 m; Gothic, Colorado, 2915 m; Glacier National Park, Montana, 976 m; Centennial, Wyoming, 3175 m; and Pinedale, Wyoming, 2386 m). Derwent et al. (2013) found that at Mace Head, a site on the west coast of Ireland, which frequently experiences air masses with minimal European influence, the measured monthly $O_3$ concentrations during the arrival of these air masses were observed to have increased between 1987 and 2008, before leveling off and decreasing. The authors did not attempt to discern whether these trends were due to changes in transport patterns, upwind emissions, or climate/meteorological phenomena. The large decreases in US emissions make it unlikely that long-range transport from the US to the EU is a key contributor to the upward shifts in the lower concentrations observed at some EU sites. Model simulations with increasing inflow from the US were not consistent with observations across Europe (Vautard et al., 2006). Overall, the evidence for long-range transport significantly impacting trends across the $O_3$ distribution is mixed and indicates that to the extent that long-range transport has affected trends, the impacts are not ubiquitous.

Climate change also has the potential to impact $O_3$ trends and could be a contributing factor to the increasing low $O_3$ concentrations, as well as an offsetting factor to decreases in high $O_3$ concentrations through changes in meteorology (e.g., UV insolation, temperature, relative humidity, and transport patterns), emissions (e.g., biogenics (Steiner et al., 2006; Zeng et al., 2008; Nolte et al., 2008), wildfires (Vautard et al., 2007; Jaffe and Widger, 2012; Keywood et al., 2013), and methane (Fiore et al., 2002; West et al., 2006; Nolte et al., 2008; Clifton et al., 2014)), or frequency and magnitude of stratospheric intrusions (Zeng et al., 2008). There have been a large number of studies that characterize potential $O_3$ increases caused by future climate-driven meteorological changes (Steiner et al., 2006; Tagaris et al., 2007; Wu et al., 2008; Zeng et al., 2008; Nolte et al., 2008; Doherty et al., 2013; Fann et al., 2015). Some investigations have looked at correlations between changing meteorological parameters and $O_3$ in the recent past (Camalier et al., 2007; Leibensperger et al., 2008; Bloomer et al., 2009; Oswald et al., 2015; Jhun et al., 2015). Many of these studies focus

on future climate change. However, there is some evidence (e.g., Leibensperger et al., 2008) that climate change may have already contributed to current $O_3$ trends through one or more of these pathways.

While we have not attempted for EU and US sites to definitively attribute the drivers for the predominant changing $O_3$ distribution pattern (i.e., Trend Type 1) observed in this study, it is likely that the decreases we observe in high $O_3$ concentrations are largely driven by the substantial decreases in local and regional precursor emissions that have occurred over the past several decades in these regions. Increases in the magnitude of the low $O_3$ concentrations is most likely caused by a combination of (1) decreasing NOx scavenging from these large emissions reductions, (2) increases in long-range transport from Asia, and (3) meteorological and natural emissions changes that have occurred due to climate. While we cannot quantitatively assess which of these factors has had the greatest impact on increases in the magnitude of the low concentrations, there is consistent modeling and observational evidence that large regional NOx reductions lead to the types of spatial and temporal patterns of increasing low $O_3$ concentrations observed in this study. In addition, long-range transport, when it does contribute to enhancing $O_3$ concentrations, is likely to have the most impact on trends in the Western US, with less substantial impact on trends in the Eastern US and Europe.

### 4.2. Implications of changes in mid-range concentrations

Various investigators have reported that the annual average and seasonal average concentrations are rising at urban sites (e.g., Paoletti et al., 2014; Sicard et al., 2016), particularly during the winter. In this study, as indicated in Section 3.1, the majority of the EU and US sites exhibited Trend Type 1 characteristics and were mostly classified as Trend Type 1a (increasing median). Thus, we observed increasing trends in the annual median (i.e., $50^{th}$ percentile) of all hourly concentrations at many sites in the EU and US, as indicated by the number of occurrences of Trend Type 1a sites (Tables 1 and 2). While the mid-range concentrations at EU and US sites generally corresponded to concentrations between 20 and 40 ppb, there was a much wider range of concentrations at sites in China. Median concentrations at some sites in mainland China were in the range 30–50 ppb, while in Hong Kong, median values were generally below 20 ppb, and at some sites between 5 and 10 ppb. While EU and the US have experienced NOx emissions reductions over decades, China has exhibited increases until recently. These two factors indicate that the drivers of increasing mid-range concentrations in the EU and US differ from those causing increases in mid-range $O_3$ concentrations in mainland China and Hong Kong, China.

With substantial resources devoted to reducing air pollution, policymakers, researchers, and the public anticipate that emissions reductions will result in reduced risk to human health and vegetation. As indicated in this study, as well as by other investigators, not all human health and vegetation exposure metrics behave in a similar manner as emissions change. Depending upon the specific exposure metrics selected for assessing the reduction of potential human health and vegetation impacts, different conclusions could be reached concerning the assessment of emission control strategies. While decreasing trends were calculated in select human health (e.g., A4DMA8 and SOMO35) and vegetation (e.g., W126 and AOT40) metrics at some EU and US sites, this frequently coincided with increasing annual median $O_3$ concentrations (Tables 4 and 5). In addition, mean concentrations have also been reported to be increasing in the literature (Paoletti et al., 2014; Sicard et al., 2016). Paoletti et al. (2014) compared $O_3$ trends during the period 1990–2010, using monitoring data from urban and rural sites from the European Environment Agency and the US Environmental Protection Agency. Ozone annual averages increased at both urban and rural sites, with a faster rate of increase for urban centers. Besides increases in annual average concentrations, monthly average concentrations also increase at some monitoring sites. Fig. 8 illustrates the trend patterns for monthly average concentrations, annual SOMO35, and annual A4MDA8 exposure metrics at an urban site in Suffolk County, New York. The monthly average concentrations increased for seven (January–April and October–December) of the 12 months, while the two human health metrics decreased. For assessing the effects of overall $O_3$ changes from anthropogenic emissions or climate-driven meteorology on human health and vegetation, we caution against focusing solely on trends using mean or median concentrations. Trends in mid-range concentrations do not appear to be well associated with some exposure metrics applicable for assessing biological effects.

### 4.3. Comparing EU and US trends in metrics and concentration bins

In this study, there were fewer sites with significant trends in the exposure metrics in the EU than in the US. For example, at sites assigned to Trend Type 1a (the most common assignment at US and EU sites), 51% of the EU sites exhibited significant trends in the A4MDA8 metric compared to 84% for the US sites. Conversely, there were more occurrences of decreasing trends in A4MDA8 at US sites (i.e., 83% of Trend Type 1a sites) compared to EU sites (50% at Trend Type 1a sites). This general pattern also held for the other metrics, which were influenced to a substantial extent by high $O_3$ concentrations.

For EU and US sites assigned to the same trend type category, differences in the proportion of sites with decreasing trends in the metrics coincided with differences in absolute concentrations and trends across the $O_3$ concentration distribution. The $O_3$ distributions at US sites during the first 5 years of the trends period (i.e., before 1995) were in general shifted towards higher concentrations than the $O_3$ distributions at EU sites. As an example, Fig. 9 shows that the magnitude of the maximum hourly average $O_3$ concentrations in the first five years of the trend period was generally greater at US sites than EU sites within each of the trend type categories except for no trend. In addition, there was a substantially larger percentage of US sites that exhibited decreasing trends over a larger range of concentration bins compared to EU sites. For almost all concentration bins above 35 ppb, a larger proportion of US sites had decreasing trends in a specific bin than the EU sites, and almost no EU sites had decreasing trends in bins above 120 ppb (Fig. 10). Taken together, these findings indicate that in the 1980s and early 1990s, when $O_3$ measurement records used in this analysis began, $O_3$ concentrations were generally higher at the US sites compared to the EU sites analyzed. Over the past several decades, the frequency of $O_3$ concentrations in the highest $O_3$ bins has decreased at more of the US sites than the EU sites, which may be due to both the different distribution of starting concentrations at the US and EU sites analyzed, as well as differences in local and regional $O_3$ precursor emission reductions over the measurement time periods.

The magnitude of trends occurring at Trend Type 1a and 1b sites was assessed based on whether a site assigned to these trend types exhibited significant trends in 95th, 98th, 99th and 100th percentiles. Assessment of the trends in these percentiles determined whether a significant trend in high $O_3$ concentrations (a requirement for assignment to Trend Type 1a or 1b) was confined to a change in the $O_3$ concentrations occurring during a relatively small number of hours (e.g., 1% of all hours in a year in the case of the 99th percentile), or whether the change in high concentrations affected a relatively larger number of hours with relatively higher $O_3$ concentrations (i.e., 5% of all hours in the case of the 95th percentile).

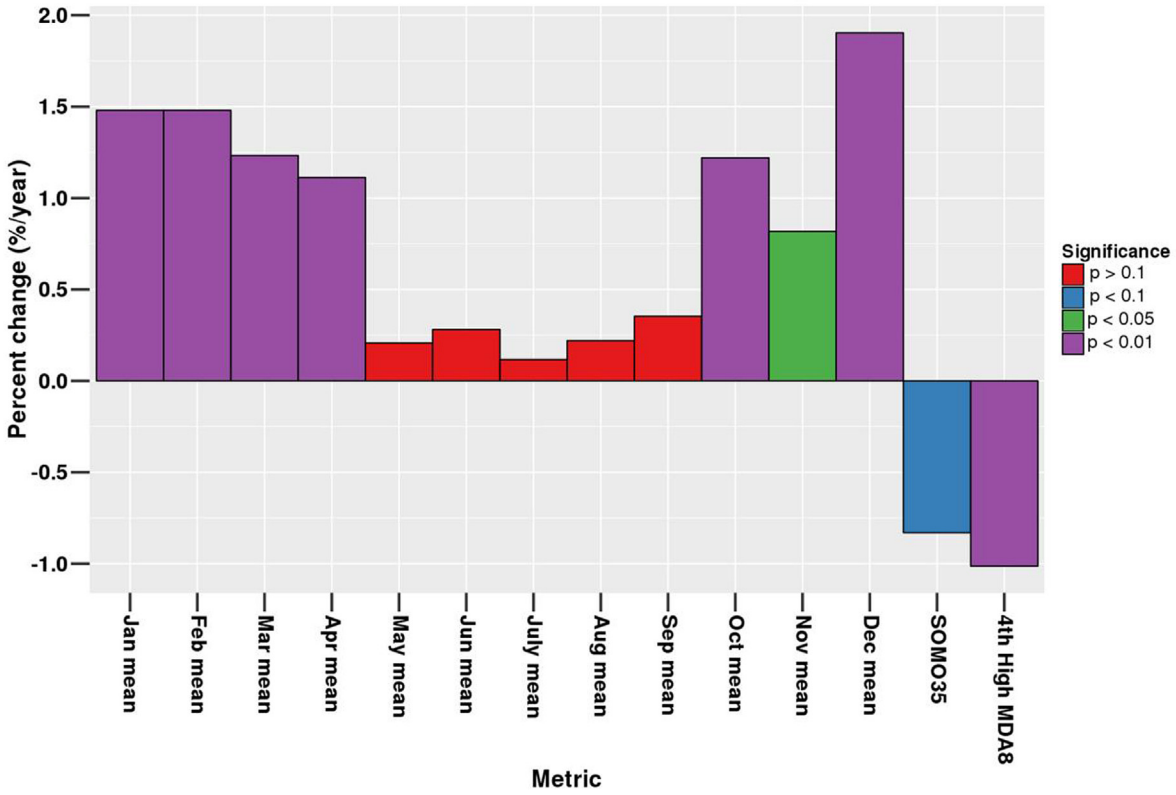


**Fig. 8.** The Theil-Sen trend (%/year) in monthly average concentrations and the annual SOMO35 and 4th highest MDA8 human health metrics (A4MDA8) for an urban site for 1980–2014 in Suffolk County, New York (EPA AQS ID: 361030002-1). For this study, $p < 0.05$ is used to determine significance using the Mann-Kendall test.

Table A.13 shows the proportion of Trend Type 1a and 1b sites with simultaneous significant trends across the high percentiles for EU and US sites separately. For the EU sites, the 95th, 98th, 99th and 100th percentiles all decreased at only 13% of the Trend Type 1a sites compared to 65% of US sites. Thus, at US sites assigned to Trend Type 1a and 1b categories, the change in high concentrations affected a relatively larger number of hours with relatively higher initial $O_3$ concentrations than the EU sites. Sites which experienced decreasing trends in high concentrations that included a larger number of hours were substantially more likely to have decreasing trends in the majority of exposure metrics; this occurred more frequently across the US sites. The lower magnitude of the higher concentrations and the lower number of hours associated with decreasing trends in these concentrations for the EU sites appear to contribute to the relatively smaller number of significant trends for the various metrics compared with US sites assigned to the same trend type category.

### 4.4. Exploration of causes of Chinese trends and policy implications

The changes in $O_3$ concentration distribution at the Chinese sites were most commonly associated with shifts towards higher concentrations, with the result that the metrics either increased in magnitude or showed no trend. Although NOx emissions reductions occurred over a short time frame toward the end of the study period, mainland China and Hong Kong exhibited increasing trends in many of the exposure metrics. Although speculative, possible reasons for not observing significant trend reductions in the exposure metrics in China may be associated with the need for a longer period than six years (2010–2015) for emission changes to influence the metric trend patterns. In addition, the scarcity of monitoring stations could possibly contribute to lack of clear trend

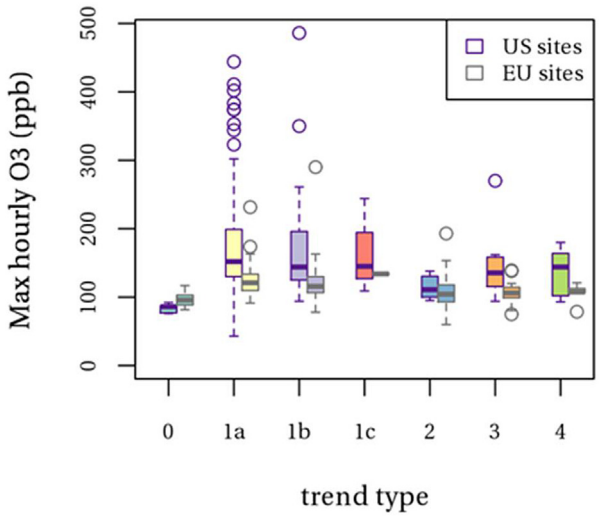


**Fig. 9.** Comparison of the distribution across sites of the maximum hourly $O_3$ concentrations in the first five years of the trend record in the US and EU for various trend types.

patterns. Year-to-year variability of meteorology could be a large factor in not observing decreases in the exposure metrics. In addition, further reductions in NOx levels may be required before decreasing trends are observed. At many of the Chinese sites, $O_3$ formation is sensitive to VOCs rather than NOx; VOCs have been increasing in mainland China (Ohara et al., 2007).

For assessing the effectiveness of emission controls in China (and elsewhere) in the near-term, it is important to identify how

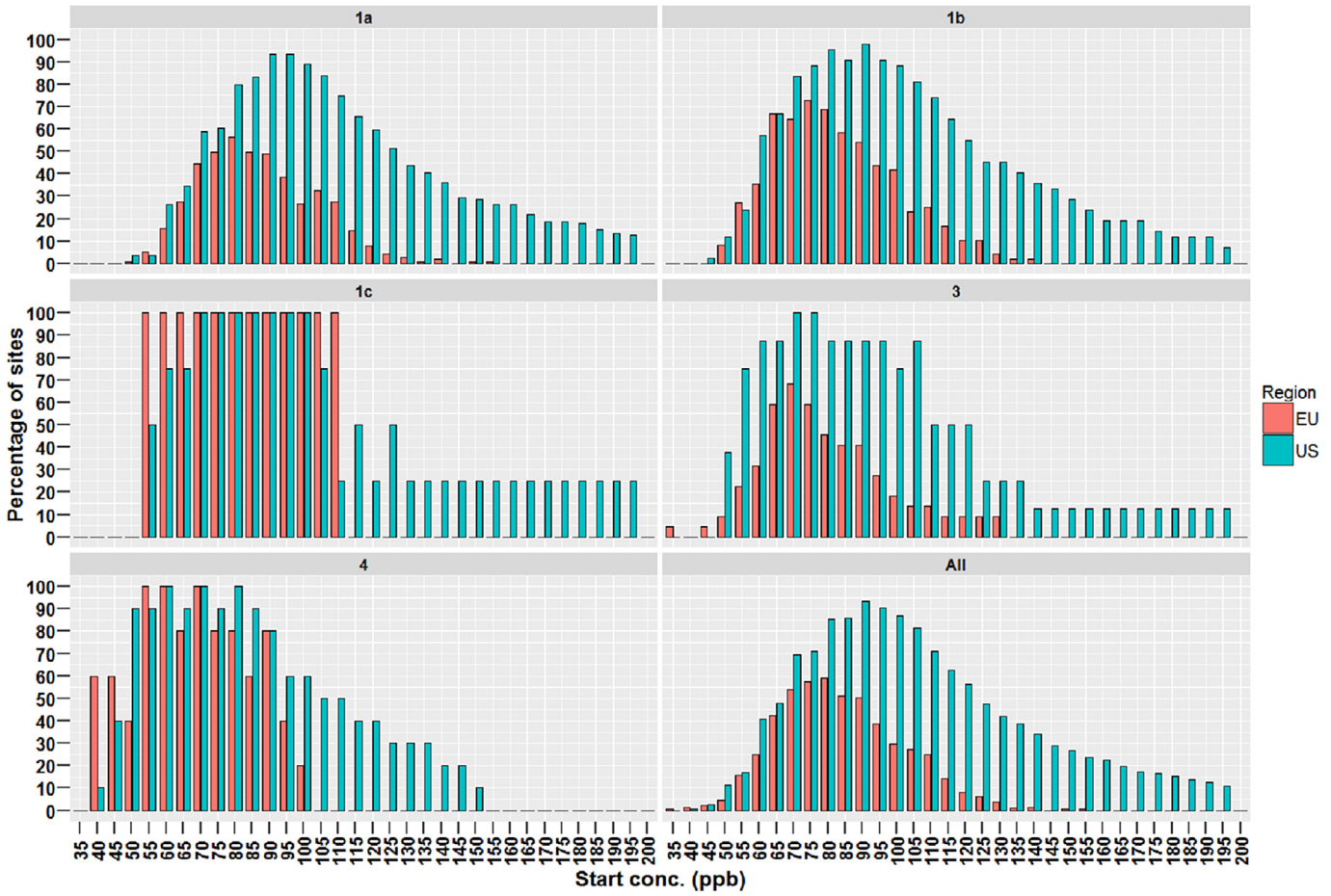


**Fig. 10.** Comparison of the proportion of all EU and US sites with decreasing trends in concentration bins above 35 ppb by trend type.

metrics selected to make such an assessment relate to those parts of the $O_3$ distribution that are influenced by changes in emissions reductions. In addition, rather than focusing on an annual period when identifying parts of the distribution initially affected, one might wish to assess whether changes occur during specific months. For example, unlike for the EU and US $O_3$ monitoring sites, where the highest concentrations generally occur during summer months (EEA, 2013; US EPA, 2014a), in China, the peak month of surface $O_3$ differs by latitude and region, changing from October in the Pearl River Delta to May in the Yangtze River Delta and to June in the North China Plain (Wang et al., 2011). The Asian summer monsoon results in reduced $O_3$ concentrations during the months of July and August.

### 4.5. Conclusions and recommendations

Understanding the relationship between exposure metrics defined to assess $O_3$ human health and vegetation impacts and changes in the distribution of hourly $O_3$ concentrations is necessary to both identify effective methods to reduce these impacts, and to evaluate the effectiveness of implemented mitigation strategies. In this work, we calculated the response of 14 human health and vegetation $O_3$ metrics to long-term trends across the $O_3$ distribution at 481 sites in the EU, US, and China. Specifically, sites were categorized into different 'trend types' according to trends in relatively low, moderate, and high hourly concentrations. Changes in the magnitude of human health and vegetation metrics, which is determined by different parts of the concentration distribution, were then compared across different trend types to understand how different changes in the concentration distribution affect different metrics.

The focus of our analyses was to assess how changes in emissions of $O_3$ precursors affect the $O_3$ distribution profile, subsequently how these changes affect trends in bins of data, and how changes in the bins affects the human health and vegetation exposure metrics. The time period selected for assessing trend patterns is important. Studies using different (and particularly shorter) time periods (e.g., 1990–2002 by Vautard et al., 2006; Jonson et al., 2006, 1996–2005 by Wilson et al., 2012) to assess trends in $O_3$ concentrations may derive different results from studies using longer time periods due to a larger influence of inter-annual variability resulting from the shorter time period, and the different extent to which drivers of $O_3$ variability may have changed over an assessment period. In our study, the minimum 20-year period selected to assess trends at EU (i.e., data between at least 1994 and 2013) and US (1995–2014) sites helped to maximize the ability to distinguish long-term trends from inter-annual variability. In studies performed by other investigators, subsets of these periods have been selected.

In the EU and US, there have been substantial reductions in $O_3$ precursor emissions over the last few decades, and at the sites analyzed, the most common trend type calculated was the reduction in the frequency of both relatively high and low concentrations, and the compression of the distribution towards the center. This predominant pattern of temporal change at the EU and US sites is consistent with large regional $NO_x$ emission reductions. The

responses of the 14 metrics to this type of change in the $O_3$ concentration distribution were varied. Those metrics determined to a greater extent by relatively high concentrations were most likely to have decreased, while the trends in metrics determined by combinations of moderate, low, and high concentrations were more varied and were less frequently significant. The trend in the latter metrics was dependent on the balance of opposing changes in the high and low concentrations. The frequency of significant trends was lower at EU sites, which was associated with the lower initial magnitude of high concentrations, and a lower number of hours associated with decreasing trends in high concentrations compared to the US sites.

In contrast to decreasing emissions in the EU and US, emissions of NOx have increased until recently in mainland China. Conversely, in Hong Kong, there have been large reductions in local emissions of both NOx and VOC since 1997. However, peak ambient $O_3$ concentrations have not decreased due to the contribution of long-range transport from increasing $O_3$ levels from mainland China (Xue et al., 2014). NOx emissions in China peaked around 2010–2011 and have since decreased (Duncan et al., 2016). Distribution changes at sites in China were most commonly associated with shifts towards higher concentrations.

The variety of trend patterns associated with this set of human health and vegetation metrics indicates that, depending upon the specific metrics selected for assessing emission control strategies, different conclusions may be reached. The results presented in this work emphasize the necessity to consider changes occurring across the entire $O_3$ distribution rather than focusing solely on mean or median $O_3$ concentrations. Trends that focus on mid-range concentrations may not be the most optimum indicators of overall changes in anthropogenic emissions, biological effects, or climate-driven meteorology. For assessing emission controls in China, the recent reductions in $O_3$ precursor emissions highlight the importance of understanding how changes in the patterns of $O_3$ distributions influence changes in the magnitude of $O_3$ metrics. An important aspect of our study is the universal applicability of the relationships between patterns of $O_3$ distribution changes and $O_3$ exposure metric trends across countries which experience substantial increases or decreases in precursor emissions. The identification of changes in the $O_3$ distribution and how these changes influence $O_3$ exposure metrics is an important step towards understanding the linkage between changes in drivers of $O_3$ variability and changes in the magnitude of human health and vegetation metrics.

## Acknowledgment

We wish to acknowledge the assistance of Mr. Nick Mangus, US EPA's Office of Air Quality Policy and Standards, for providing technical insight concerning $O_3$ monitoring sites in the US. One of the authors (ASL) wishes to acknowledge his company, A.S.L. & Associates, for providing the necessary resources that allowed him to participate in the study. The author (XX) from the Chinese Academy of Meteorological Sciences acknowledges the support from the National Science Foundation of China (No. 41330422). The $O_3$ observations at Mt. Waliguan, Shangdianzi, and Longfengshan are supported by the China Meteorological Administration. The Hong Kong authors (TW and LZ) acknowledge the support from the Hong Kong Research Grants Council (PolyU 153042/15E). The $O_3$ observations at Hok Tsui are supported by The Hong Kong Polytechnic University (Project No. G-S023). Two of the authors (HS and BW) wish to note that although this work has been reviewed and approved for publication by the US Environmental Protection Agency (EPA), it does not reflect the views and policies of the agency.

## Appendices A–E. Supplementary data

Supplementary data related to this article can be found at http://dx.doi.org/10.1016/j.atmosenv.2016.12.025.

## References

Avnery, S., Mauzerall, D.L., Liu, J., Horowitz, L.W., 2011. Global crop yield reductions due to surface ozone exposure: 1. Year 2000 crop production losses and economic damage. Atmos. Environ. 45, 2284–2296.

Bloomer, B.J., Stehr, J.W., Piety, C.A., Salawitch, R.J., Dickerson, R.R., 2009. Observed relationships of ozone air pollution with temperature and emissions. Geophys. Res. Lett. 36, L09803. http://dx.doi.org/10.1029/2009GL037308.

Butler, T.J., Vermeylen, F.M., Rury, M., Likens, G.E., Lee, B., Bowker, G.E., McCluney, L., 2011. Response of ozone and nitrate to stationary source NOx emission reductions in the eastern USA. Atmos. Environ. 45 (5), 1084–1094.

Camalier, L., Cox, W., Dolwick, P., 2007. The effects of meteorology on ozone in urban areas and their use in assessing ozone trends. Atmos. Environ. 41, 7127–7173.

Chan, E., 2009. Regional ground-level ozone trends in the context of meteorological influences across Canada and the eastern United States from 1997 to 2006. J. Geophys. Res.-Atmos. 114, D05301.

Chan, E., Vet, R.J., 2010. Baseline levels and trends of ground level ozone in Canada and the United States. Atmos. Chem. Phys. 10 (18), 8629–8647.

Clifton, O.E., Fiore, A.M., Correa, G., Horowitz, L.W., Naik, V., 2014. Twenty-first century reversal of the surface ozone seasonal cycle over the northeastern United States. Geophy. Res. Lett. 41 (20), 7343–7350.

CLRTAP, 2015. Mapping Critical Levels for Vegetation, Chapter III of Manual on Methodologies and Criteria for Modelling and Mapping Critical Loads and Levels and Air Pollution Effects, Risks and Trends. UNECE Convention on Long-range Transboundary Air Pollution accessed on (15.12.16) on web at www.icpmapping.org.

Cooper, O.R., Parrish, D.D., Stohl, A., Trainer, M., Nedelec, P., Thouret, V., Cammas, J.P., Oltmans, S.J., Johnson, B.J., Tarasick, D., Leblanc, T., McDermid, I.S., Jaffe, D., Gao, R., Stith, J., Ryerson, T., Aikin, K., Campos, T., Weinheimer, A., Avery, M.A., 2010. Increasing springtime ozone mixing ratios in the free troposphere over western North America. Nature 463 (7279), 344–348.

Cooper, O.R., Gao, R.S., Tarasick, D., Leblanc, T., Sweeney, C., 2012. Long-term ozone trends at rural ozone monitoring sites across the United States, 1990–2010. J. Geophys. Res. Atmos. 117, D22. http://dx.doi.org/10.1029/2012JD018261.

De Smedt, I., Stavrakou, T., Hendrick, F., Danckaert, T., Vlemmix, T., Pinardi, G., Theys, N., Lerot, C., Gilelen, C., Vigouroux, C., Hermans, C., Fayt, C., Veefkind, J.P., Müller, J.-F., Van Roozendael, M., 2015. Diurnal, seasonal, and long-term variation of global formaldehyde columns inferred from combined OMI and GOME-2 observations. Atmos. Chem. Phys. 15, 12519–12545. http://dx.doi.org/10.5194/acp-15-12519-2015.

Derwent, R.G., 2008. New directions: prospects for regional ozone in North-west Europe. Atmos. Environ. 42, 1958–1960. http://dx.doi.org/10.1016/j.atmosenv.2007.11.028.

Derwent, R., Manning, A., Simmonds, P., Gerard Spain, T., O'Doherty, S., 2013. Analysis and interpretation of 25 years of ozone observations at the mace Head atmospheric research station on the Atlantic ocean coast of Ireland from 1987 to 2012. Atmos. Environ. 80, 361–368.

Derwent, R.G., Utembe, S.R., Jenkin, M.E., Shallcross, D.E., 2015. Tropospheric ozone production regions and the intercontinental origins of surface ozone over Europe. Atmos. Environ. 112, 216–224. http://dx.doi.org/10.1016/j.atmosenv.2015.04.049.

Ding, A., Wang, T., 2006. Influence of stratosphere-to-troposphere exchange on the seasonal cycle of surface ozone at Mount Waliguan in western China. Geophys. Res. Lett. 33, L03803. http://dx.doi.org/10.1029/2005GL024760.

Doherty, R.M., Wild, O., Shindell, D.T., Zeng, G., MacKenzie, I.A., Collins, W.J., Fiore, A.M., Stevenson, D.S., Dentener, F.J., Schultz, M.G., Hess, P., Derwent, R.G., Keating, T.J., 2013. Impacts of climate change on surface ozone and intercontinental ozone pollution: a multi-model study. J. Geophys. Res. Atmos. 118, 3744–3763. http://dx.doi.org/10.1002/jgrd.50266.

Downey, N., Emery, C., Jung, J., Sakulyanontvittaya, T., Hebert, L., Blewitt, D., Yarwood, G., 2015. Emission reductions and urban ozone responses under more stringent US standards. Atmos. Environ. 101, 209–216.

Duncan, B.N., Lamsal, L.N., Thompson, A.M., Yoshida, Y., Lu, Z., Streets, D.G., Hurwitz, M.M., Pickering, K.E., 2016. A space-based, high-resolution view of notable changes in urban NOx pollution around the world (2005–2014). J. Geophys. Res. Atmos. 121, 976–996. http://dx.doi.org/10.1002/2015JD024121.

EEA, 2009. Assessment of Ground-level Ozone in EEA Member Countries, with a Focus on Long-term Trends. EEA Technical report No 7/2009.

EEA, 2013. Air Pollution by Ozone across Europe during Summer 2012: Overview of Exceedances of EC Ozone Threshold Values for April–september 2012. EEA Technical Report No. 3/2013. European Environment Agency. available at: http://www.eea.europa.eu/publications/air-pollution-by-ozone-across-EU-2012/download.

EEA, 2015. EU Emission Inventory Report 1990-2013 under the UNECE Convention on Long-range Transboundary Air Pollution (LRTAP). EEA technical report No 8/2015. European Environment Agency. available at: http://www.eea.europa.eu//publications/lrtap-emission-inventory-report.

European Commission, 2013. Guidance on the Commission Implementing Decision Laying Down Rules for Directives 2004/107/EC and 2008/50/EC of the European Parliament and of the Council as Regards the Reciprocal Exchange of Information and Reporting on Ambient Air. European Commission Report. available at: http://ec.europa.eu/environment/air/quality/legislation/pdf/IPR_guidance1.pdf.

European Council Directive 2008/50/EC, 21st May 2008. On Ambient Air Quality and Cleaner Air for Europe. L 152/1.

Fann, N., Nolte, C.G., Dolwick, P., Spero, T.L., Brown, A.C., Phillips, S., Anenberg, S., 2015. The geographic distribution and economic value of climate change-related ozone health impacts in the United States in 2030. J. Air Waste Manag. Assoc. 65 (5), 570–580.

Fiore, A.M., Jacob, D.J., Field, B.D., Streets, D.G., Fernandes, S.D., Jang, C., 2002. Linking ozone pollution and climate change: the case for controlling methane. Geosphys. Res. Lett. 29 (19), 1919. http://dx.doi.org/10.1029/2002GL015601.

Fiore, A.M., Dentener, F.J., Wild, O., Cuvelier, C., Schultz, M.G., Hess, P., Textor, C., Schulz, M., Doherty, R.M., Horowitz, L.W., MacKenzie, I.A., Sanderson, M.G., Shindell, D.T., Stevenson, D.S., Szopa, S., Van Dingenen, R., Zeng, G., Atherton, C., Bergmann, D., Bey, I., Carmichael, G., Collins, W.J., Duncan, B.J., Faluvegi, G., Folberth, G., Gauss, M., Gong, S., Hauglustaine, D., Holloway, T., Isaksen, I.S.A., Jacob, D.J., Jonson, J.E., Kaminski, J.W., Keating, T.J., Lupu, A., Marmer, E., Montanaro, V., Park, R.J., Pitari, G., Pringle, K.J., Pyle, J.A., Schroeder, S., Vivanco, M.G., Wind, P., Wojcik, G., Wu, S., Zuber, A., 2009. Multimodel estimates of intercontinental source-receptor relationships for ozone pollution. J. Geophys. Res. 114, D04301. http://dx.doi.org/10.1029/2008JD010816.

Ge, B.Z., Xu, X.B., Lin, W.L., Li, J., Wang, Z.F., 2012. Impact of the regional transport of urban Beijing pollutants on downwind areas in summer: ozone production efficiency analysis. Tellus B 64, 17348. http://dx.doi.org/10.3402/tellusb.v64i0.17348.

Gilliland, A.B., Hogrefe, C., Pinder, R.W., Godowitch, J.M., Foley, K.M., Rao, S.T., 2008. Dynamic evaluation of regional air quality models: assessing changes in O3 stemming from changes in emissions and meteorology. Atmos. Environ. 42, 5110–5123.

Granier, C., Bessagnet, B., Bond, T., D'Angiola, A., van der Gon, H.D., Gregory, J., Frost, G.J., Heil, A., Kaiser, J.W., Kinne, S., Klimont, Z., Kloster, S., Lamarque, J.F., Liousse, C., Masui, T., Meleux, F., Mieville, A., Ohara, T., Raut, J.C., Riahi, K., Schultz, M.G., Smith, S.J., Thompson, A., Aardenne, J.V., Werf, G.R., Vuuren, D.P., 2011. Evolution of anthropogenic and biomass burning emissions of air pollutants at global and regional scales during the 1980–2010 period. Clim. Change 109, 163–190. http://dx.doi.org/10.1007/s10584-011-0154-1.

Hogrefe, C., Hao, W., Zalewsky, E.E., Ku, J.-Y., Lynn, B., Rosenzweig, C., Schultz, M.G., Rast, S., Newchurch, M.J., Wang, L., Kinney, P.L., Sistla, G., 2011. An analysis of long-term regional-scale ozone simulations over the Northeastern United States: variability and trends. Atmos. Chem. Phys. 11, 567–582.

Jaffe, D.A., Widger, W.L., 2012. Ozone production from wildfires: a critical review. Atmos. Environ. 51, 1–10.

Jaffe, D., McKendry, I., Anderson, T., Price, H., 2003. Six 'new' episodes of trans-Pacific transport of air pollutants. Atmos. Environ. 37, 391–404.

Jassby, A.D., Cloern, J.E., 2016. wq: Some tools for exploring water quality monitoring data. R. package version 0.4.7. http://cran.r-project.org/package=wq.

Jenkin, M.E., 2008. Trends in ozone concentration distributions in the UK since 1990: local regional and global influences. Atmos. Environ. 42, 5434–5445.

Jhun, I., Coull, B.A., Schwartz, J., Hubbell, B., Koutrakis, P., 2015. The impact of weather changes on air quality and health in the United States in 1994-2012. Environ. Res. Letters 10, 084009.

Jonson, J.E., Simpson, D., Fagerli, H., Solberg, S., 2006. Can we explain the trends in European ozone levels? Atmos. Chem. Phys. 6, 51–66.

JRC-AQUILA, 2013. JRC-AQUILA Position Paper: assessment on siting criteria, classification and representativeness of air quality monitoring stations. Available at: http://ec.europa.eu/environment/air/pdf/SCREAM%20final.pdf.

Karlsson, P.E., Tang, L., Sundberg, J., Chen, D., Lindskog, A., Pleijel, H., 2007. Increasing risk for negative ozone impacts on vegetation in northern Sweden. Environ. Pollut. 150, 96–106.

Keywood, M., Kanakidou, M., Stohl, A., Dentener, F., Grassi, G., Meyer, C.P., Torseth, K., Edwards, D., Thompson, A.M., Lohmann, U., Burrows, J., 2013. Fire in the air: biomass burning impacts in a changing climate, critical reviews in environ. Sci. Technol. 43 (1), 40–83.

Koumoutsaris, S., Bey, I., 2012. Can a global model reproduce observed trends in summertime surface ozone levels? Atmos. Chem. Phys. 12, 6983–6998.

Krotkov, N.A., McLinden, C.A., Li, C., Lamsal, L.N., Celarier, E.A., Marchenko, S.V., Swartz, W.H., Bucsela, E.J., Joiner, J., Duncan, B.N., Boersma, K.F., Veefkind, J.P., Levelt, P.F., Fioletov, V.E., Dickerson, R.R., He, H., Lu, Z., Streets, D.G., 2016. Aura OMI observations of regional SO2 and NO2 pollution changes from 2005 to 2015. Atmos. Chem. Phys. 16, 4605–4629.

Kurokawa, J., Ohara, T., Morikawa, T., Hanayama, S., Janssens-Maenhout, G., Fukui, T., Kawashima, K., Akimoto, H., 2013. Emissions of air pollutants and greenhouse gases over Asian regions during 2000–2008: regional Emission inventory in Asia (REAS) version 2. Atmos. Chem. Phys. 13, 11019–11058. http://dx.doi.org/10.5194/acp-13-11019-2013.

Lamsal, L.N., Duncan, B.N., Yoshida, Y., Krotlov, N.A., Pickering, K.E., Streets, D.G., Lu, Z., 2015. U.S. NO2 trends (2005–2013): EPA air quality System (AQS) data versus improved observations from the ozone monitoring instrument (OMI). Atmos. Environ. 110, 130–143.

Langford, A.O., Senff, C.J., Alcarez, R.J., Brioude, J., Cooper, O.R., Holloway, J.S., Lin, M., Marchbanks, J.S., Pierce, R.B., Sandberg, S.P., Weickmann, A.M., Willams, E.J., 2015. An overview of the 2013 Las Vegas Ozone Study (LVOS): impact of stratospheric intrusions and long-range transport on surface air quality. Atmos. Environ. 109, 305–322.

Lefohn, A.S., Hazucha, M.J., Shadwick, D., Adams, W.C., 2010a. An alternative form and level of the human health ozone standard. Inhal. Toxicol. 22 (12), 999–1011.

Lefohn, A.S., Shadwick, D., Oltmans, S.J., 2010b. Characterizing changes in surface ozone levels in metropolitan and rural areas in the United States for 1980–2008 and 1994–2008. Atmos. Environ. 44 (39), 5199–5210.

Leibensperger, E.M., Mickley, L.J., Jacob, D.J., 2008. Sensitivity of US air quality to mid-latitude cyclone frequency and implications of 1980–2006 climate change. Atmos. Chem. Phys. 8, 7075–7086.

Li, Q., Jacob, D.J., Bey, I., Palmer, P.I., Duncan, B.N., Field, B.D., Martin, R.V., Fiore, A.M., Yantosca, R.M., Parrish, D.D., Simmonds, P.G., Oltmans, S.J., 2002. Transatlantic transport of pollution and its effects on surface ozone in Europe and North America. J. Geophys. Res. 107 (D13) http://dx.doi.org/10.1029/2001JD001422.

Li, J.F., Lu, K.D., Lv, W., Li, J., Zhong, L.J., Ou, Y., Chen, D., Huang, X., Zhang, Y., 2014. Fast increasing of surface ozone concentrations in Pearl River Delta characterized by a regional air quality monitoring network during 2006-2011. J. Environ. Sci. 26 (1), 23–36.

Lin, X., Trainer, M., Liu, S.C., 1988. On the nonlinearity of the tropospheric ozone production. J. Geophys. Res. 93 (D12), 15879–15888. http://dx.doi.org/10.1029/JD093iD12p15879.

Lin, W., Xu, X., Zhang, X., Tang, J., 2008. Contributions of pollutants from North China plain to surface ozone at the Shangdianzi GAW station. Atmos. Chem. Phys. 8, 5889–5898.

Lin, M., Fiore, A.M., Horowitz, L.W., Cooper, O.R., Naik, V., Holloway, J., Johnson, B.J., Middlebrook, A.M., Oltmans, S.J., Pollack, I.B., Ryerson, T.B., Warner, J.X., Wiedinmyer, C., Wilson, J., Wyman, B., 2012. Transport of Asian ozone pollution into surface air over the western United States in spring. J. Geophys. Res. 117, D00V07. http://dx.doi.org/10.1029/2011JD016961.

Lin, M., Horowitz, L.W., Cooper, O.R., Tarasick, D., Conley, S., Iraci, L.T., Johnson, B., Leblanc, T., Petropavlovskikh, I., Yates, E.L., 2015. Revisiting the evidence of increasing springtime ozone mixing ratios in the free troposphere over western. North Am. geophys. Res. Lett. 42, 8719–8728. http://dx.doi.org/10.1002/2015GL065311.

Liu, S.C., Trainer, M., Fehsenfeld, F.C., Parrish, D.D., Williams, E.J., Fahey, D.W., Hübler, G., Murphy, P.C., 1987. Ozone production in the rural troposphere and the implications for regional and global ozone distributions. J. Geophys. Res. 92 (D4), 4191–4207. http://dx.doi.org/10.1029/JD092iD04p04191.

Lu, Q., Zheng, J., Ye, S., Shen, X., Yuan, Z., Yin, S., 2013. Emission trends and source characteristics of SO2, NOx, PM10 and VOCs in the Pearl River Delta region from 2000 to 2009. Atmos. Environ. 76, 11–20. http://dx.doi.org/10.1016/j.atmosenv.2012.10.062.

Lu, Z., Streets, D.G., de Foy, B., Lamsal, L.N., Duncan, B.N., Xing, J., 2015. Emissions of nitrogen oxides from US urban areas: estimation from Ozone Monitoring Instrument retrievals for 2005–2014. Atmos. Chem. Phys. 15, 10367–10383. http://dx.doi.org/10.5194/acp-15-10367-2015, 2015.

Ma, J., Tang, J., Zhou, X., Zhang, X., 2002. Estimates of the chemical budget for ozone at Waliguan observatory. J. Atmos. Chem. 41, 21–48. http://dx.doi.org/10.1023/A:1013892308983, 2002.

Maas, R., Grennfelt, P. (Eds.), 2016. Towards Cleaner Air. Scientific Assessment Report 2016. EMEP Steering Body and Working Group on Effects of the Convention on Long-Range Transboundary Air Pollution, Oslo xx+50pp.

Malley, C.S., Heal, M.R., Mills, G., Braban, C.F., 2015. Trends and drivers of ozone human health and vegetation impact metrics from UK EMEP supersite measurements (1990-2013). Atmos. Chem. Phys. 15 (8), 4025–4042.

Mann, H.B., 1945. Nonparametric tests against trend. Econometrica 13, 245–259.

Mijling, B., van der A, R.J., Zhang, Q., 2013. Regional nitrogen oxides emission trends in East Asia observed from space. Atmos. Chem. Phys. 13, 12003–12012. http://dx.doi.org/10.5194/acp-13-12003-2013.

Monks, P.S., Archibald, A.T., Colette, A., Cooper, O., Coyle, M., Derwent, R., Fowler, D., Granier, C., Law, K.S., Mills, G.E., Stevenson, D.S., Tarasova, O., Thouret, V., von Schneidemesser, E., Sommariva, R., Wild, O., Williams, M.L., 2015. Tropospheric ozone and its precursors from the urban to the global scale from air quality to short-lived climate forcer. Atmos. Chem. Phys. 15, 8889–8973. http://dx.doi.org/10.5194/acp-15-8889-2015, 2015.

Multi-resolution Emission Inventory for China (MEIC) http://www.meicmodel.org).

Nolte, C.G., Gilliland, A.B., Hogrefe, C., Mickley, L.J., 2008. Linking global to regional models to assess future climate impacts on surface ozone levels in the United States. J. Geophys. Res. 113, D14307. http://dx.doi.org/10.1029/2007JD008497.

Ohara, T., Akimoto, H., Kurokawa, J., Horii, N., Yamaji, K., Yan, X., Hayasaka, T., 2007. An Asian emission inventory of anthropogenic emission sources for the period 1980–2020. Atmos. Chem. Phys. 7, 4419–4444. http://dx.doi.org/10.5194/acp-7-4419-2007.

Oswald, E.M., Dupigny-Giroux, L.-A., Leibensperger, E.M., Poirot, R., Merrell, J., 2015. Climate controls on air quality in the Northeastern U.S.: an examination of summertime ozone statistics during 1993-2012. Atmos. Environ. 112, 278–288.

Paoletti, E., De Marco, A., Beddows, D.C.S., Harrison, R.M., Manning, W.J., 2014. Ozone levels in European and USA cities are increasing more than at rural sites, while peak values are decreasing. Environ. Pollut. 192, 295–299.

R Core Team, 2016. R: a Language and Environment for Statistical Computing. R Foundation for Statistical Computing, Vienna, Austria. https://www.R-project.org/.

R Development Core Team, 2008. R: a Language and Environment for Statistical Computing. R Foundation for Statistical Computing, Vienna, Austria, ISBN 3-

900051-07-0. http://www.R-project.org.
REVIHAAP, 2013. Review of Evidence on Health Aspects of Air Pollution – REVIHAAP Project Technical Report. World Health Organization (WHO) Regional Office for Europe, Bonn. Available at: http://www.euro.who.int/__data/assets/pdf_file/0004/193108/REVIHAAP-Final-technical-report-final-version.pdf.
Richter, A., Burrows, J.P., Nub, H., Granier, C., Neimeier, U., 2005. Increase in tropospheric nitrogen dioxide over China observed from space. Nature 437, 129–132. http://dx.doi.org/10.1038/nature04092.
Sather, M.E., Cavender, K., 2012. Update of long-term trends analysis of ambient 8-h ozone and precursor monitoring data in the South Central U.S.; encouraging news. J. Environ. Monit. 14 (2), 666–676.
Schertz, T.L., Alexander, R.B., Ohe, D.J., 1991. The Computer Program EStimate TREND (ESTREND), a System for the Detection of Trends in Water-quality Data. Water-Resources Investigations Report 91–4040. U.S. Geological Survey. Available at: http://pubs.usgs.gov/wri/wri91-4040/pdf/wri91-4040.aug.pdf.
Sen, P.K., 1968. Estimates of the regression coefficient based on Kendall's tau. J. Amer. Stat. Ass. 63, 1379–1389.
Sicard, P., Serra, R., Rossello, P., 2016. Spatiotemporal trends in ground-level ozone concentrations and metrics in France over the time period 1999–2012. Environ. Res. 149, 122–144. http://dx.doi.org/10.1016/j.envres.2016.05.014.
Sillman, S., 1990. The relation between ozone, NOx and hydrocarbons in urban and polluted rural environments. Atmos. Environ. 33 (12), 1821–1845.
Sillman, S., Logan, J.A., Wofsy, S.C., 1990. The sensitivity of ozone to nitrogen oxides and hydrocarbons in regional ozone episode. J. Geophys. Res. 95 (D2), 1837–1851.
Simon, H., Baker, K.R., Akhtar, F., Napelenok, S.L., Possiel, N., Wells, B., Timin, B., 2013. A direct sensitivity approach to predict hourly ozone resulting from compliance with the National Ambient Air Quality Standard. Environ. Sci. Technol. 47, 2304–2313.
Simon, H., Reff, A., Wells, B., Frank, N., 2015. Ozone trends across the United States over a period of decreasing NOx and VOC emissions. Environ. Sci. Technol. 49, 186–195.
Simon, H., Wells, B., Baker, K.R., Hubbell, B., 2016. Assessing temporal and spatial patterns of observed and predicted ozone in multiple urban areas. Environ. Health. Perspect. 124, 1443–1452. http://dx.doi.org/10.1289/EHP190.
Simpson, D., Arneth, A., Mills, G., Solberg, S., Uddling, J., 2014. Ozone - the persistent menace: interactions with the N cycle and climate change. Curr. Opin. Environ. Sustain. 9–10, 9–19.
Steiner, A.L., Tonse, S., Cohen, R.C., Goldstein, A.H., Harley, R.A., 2006. Influence of future climate and emissions on regional air quality in California. J. Geophys. Res. 111, D18303. http://dx.doi.org/10.1029/2005JD006935.
Stohl, A., Trickl, T., 1999. A textbook example of long-range transport: simultaneous observation of ozone maxima of stratospheric and North American origin in the free troposphere over Europe. J. Geophys. Res. 104 (D23), 30445–30462. http://dx.doi.org/10.1029/1999JD900803.
Streets, D.G., Tsai, N.Y., Akimoto, H., Oka, K., 2001. Trends in emissions of acidifying species in Asia, 1985–1997. Water Air Soil Poll. 130, 187–192. http://dx.doi.org/10.1023/A:1013883628877.
Sun, L., Xue, L., Wang, T., Gao, J., Ding, A., Cooper, O.R., Xu, P., Wang, Z., Wang, X., Wen, L., Zhu, Y., Chen, T., Yang, L., Wang, Y., Chen, J., Wang, W., 2016. Significant increase of summertime ozone at Mt. Tai in Central Eastern China:2003-2015. Atmos. Chem. Phys. 16, 10637–10650. http://dx.doi.org/10.5194/acp-16-10637-2016. http://www.atmos-chem-phys.net/16/10637/2016/.
Tagaris, E., Manomaiphiboon, K., Liao, K.-J., Leung, L.R., Woo, J.-H., He, S., Amar, P., Russell, A.G., 2007. Impacts of global climate change and emissions on regional ozone and fine particulate matter concentrations over the United States. J. Geophys. Res. 112, D14312. http://dx.doi.org/10.1029/2006JD008262.
TF HTAP, 2010. Hemispheric Transport of Air Pollution 2010: Part a Ozone. Air Pollution Studies No. 17. Prepared by the Task Force on Hemispheric Transport of Air Pollution acting within the framework of the Convention on Long-range Transboundary Air Pollution. United Nations Economic Commission for Europe. Available at: http://www.htap.org/publications/2010_report/2010_Final_Report/HTAP%202010%20Part%20A%20110407.pdf.
Theil, H., 1950a. A rank-invariant method of linear and polynomial regression analysis. I. Proc. Kon. Ned. Akad. V. Wetensch. A 53, 386–392.
Theil, H., 1950b. A rank-invariant method of linear and polynomial regression analysis. II. Proc. Kon. Ned. Akad. V. Wetensch. A 53, 521–525.
Theil, H., 1950c. A rank-invariant method of linear and polynomial regression analysis. III. Proc. Kon. Ned. Akad. V. Wetensch. A 53, 1397–1412.
Torseth, K., Aas, W., Breivik, K., Fjaeraa, A.M., Fiebig, M., Hjellbrekke, A.G., Lund Myhre, C., Solberg, S., Yttri, K.E., 2012. Introduction to the european monitoring and evaluation programme (EMEP) and observed atmospheric composition change during 1972-2009. Atmos. Chem. Phys. 12 (12), 5447–5481.
Tripathi, O.P., Jennings, S.G., O'Dowd, C., O'Leary, B., Lambkin, K., Moran, E., O'Doherty, S., Gerard Spain, T., 2012. An assessment of the surface ozone trend in Ireland relevant to air pollution and environmental protection. Atmos. Poll. Res. 3 (3), 341–351.
UNECE, 1979. 1979 Convention on Long-range Transboundary Air Pollution. Available at: http://www.unece.org/fileadmin/DAM/env/lrtap/full%20text/1979.CLRTAP.e.pdf.
UNECE, 1999. Protocol to the 1979 Convention on Long-range Transboundary Air Pollution to Abate Acidification, Eutrophication and Ground-level Ozone. Available at: http://www.unece.org/fileadmin/DAM/env/lrtap/full%20text/1999%20Multi.E.Amended.2005.pdf.
UNECE, 2013. 1999 Protocol to Abate Acidification, Eutrophication and Ground-level Ozone to the Convention on Long-range Transboundary Air Pollution as amended on 4 May 2012. Available at: http://www.unece.org/fileadmin/DAM/env/documents/2013/air/eb/ECE.EB.AIR.114_EN.
US EPA, 2013. Integrated Science Assessment for Ozone and Related Photochemical Oxidants. EPA/600/R-10/076F. Office of Research and Development, Research Triangle Park, NC (February).
US EPA, 2014a. Health Risk and Exposure Assessment for Ozone. Final Report. EPA/452/R-14–004a, available at: http://www3.epa.gov/ttn/naaqs/standards/ozone/s_o3_2008_rea.html.
US EPA, 2014b. Policy Assessment for the Review of the Ozone National Ambient Air Quality Standards. Final Report. EPA-452/R-14-006. Office of Air Quality Planning and Standards, Research Triangle Park, NC (August).
US EPA, 2015. Our Nation's Air, Status and Trends through 2015. RTP, NC https://gispub.epa.gov/air/trendsreport/2016/.
Van Dingenen, R., Dentener, F.J., Raes, F., Krol, M.C., Emberson, L., Cofala, J., 2009. The global impact of ozone on agricultural crop yields under current and future air quality legislation. Atmos. Environ. 43, 604–618.
Vautard, R., Szopa, S., Beekmann, M., Menut, L., Hauglustaine, D.A., Rouil, L., Roemer, M., 2006. Are decadal anthropogenic emission reductions in Europe consistent with surface ozone observations? Geophys. Res. Lett. 33, L13810. http://dx.doi.org/10.1029/2006GL026080.
Vautard, R., Beekmann, M., Desplat, J., Hodzic, A., Morel, S., 2007. Air quality in Europe during the summer of 2003 as a prototype of air quality in a warmer climate. Comptes Rendus Geosci. 339, 747–763.
Walcek, C.J., Yuan, H.H., 1995. Calculated influence of temperature-related factors on ozone formation rates in the lower troposphere. J. App. Met. 34, 1056–1069.
Wang, M., Shao, M., Che1, W., Lu, S., Liu, Y., Yuan, B., Zhan, Q., Zhang, Q., Chang, C.-C., Wang, B., Zeng, L., Hu, M., Yang, Y., Li, Y., 2015. Trends of non-methane hydrocarbons (NMHC) emissions in Beijing during 2002–2013. Atmos. Chem. Phys. 15, 1489–1502.
Wang, T., Wong, H.L.A., Tang, J., Ding, A., Wu, W.S., Zhang, X.C., 2006. On the origin of surface ozone and reactive nitrogen observed at a remote mountain site in the northeastern Qinghai-Tibetan Plateau, western China. J. Geophys. Res.-Atmos. 111, D08303. http://dx.doi.org/10.1029/2005JD006527.
Wang, T., Wei, X.L., Ding, A.J., Poon, C.N., Lam, K.S., Li, Y.S., Chan, L.Y., Anson, M., 2009. Increasing surface ozone concentrations in the background atmosphere of Southern China, 1994–2007. Atmos. Chem. Phys. 9, 6217–6227. http://dx.doi.org/10.5194/acp-9-6217-2009.
Wang, Y., Zhang, Y., Hao, J., Luo, M., 2011. Seasonal and spatial variability of surface ozone over China: contributions from background and domestic pollution, 2011. Atmos. Chem. Phys. 11, 3511–3525, 2011. www.atmos-chem-phys.net/11/3511/2011/doi:10.5194/acp-11-3511-2011.
West, J., Fiore, A.M., Horowitz, J.W., Mauzerall, D.L., 2006. Global health benefits of mitigating ozone pollution with methane emission controls. Proceed. Nat. Acad. Sci. 103, 3988–3993.
Wilson, R.C., Fleming, Z.L., Monks, P.S., Clain, G., Henne, S., Konovalov, I.B., Szopa, S., Menut, L., 2012. Have primary emission reduction measures reduced ozone across Europe? An analysis of European rural background ozone trends 1996-2005. Atmos. Chem. Phys. 12, 437–454.
Wu, S., Mickley, L.J., Leibensperger, E.M., Jacob, D.J., Rind, D., Streets, D.G., 2008. Effects of 2000–2050 global change on ozone air quality in the United States. J. Geophys. Res. 113, D06302. http://dx.doi.org/10.1029/2007JD008917.
Xing, J., Pleim, J., Mathur, R., Pouliot, G., Hogrefe, C., Gan, C.-M., Wei, C., 2013. Historical gaseous and primary aerosol emissions in the United States from 1990 to 2010. Atmos. Chem. Phys. 13, 7531–7549. http://dx.doi.org/10.5194/acp-13-7531-2013.
Xing, J., Mathur, R., Pleim, J., Hogrefe, C., Gan, C.-M., Wong, D.C., Wei, C., Gilliam, R., Pouliot, G., 2015. Observations and modeling of air quality trends over 1990–2010 across the Northern Hemisphere: China, the United States and Europe. Atmos. Chem. Phys. 15, 2723–2747. http://dx.doi.org/10.5194/acp-15-2723-2015.
Xu, X., Ding, G., Li, X., Xiang, R., 1997. Study on acidic gases in the regional background air in northeastern China. China Environ. Sci. 17 (4), 345–348 (in Chinese with English abstract).
Xu, X., Ding, G., Li, X., Xiang, R., 1998. Variability and related factors of the surface O3 at Longfengshan in Northeast China. Acta Meteorol. Sinca 56 (5), 560–572 (in Chinese with English abstract).
Xu, X., Lin, W., Yan, P., Dai, X., Yu, X., 2009a. Long-term changes of acidic gases in China's Yangtze Delta and northeast plain regions in 1994-2006. Adv. Clim. Change Res. (5 Suppl. l), 5–10.
Xu, X., Liu, X., Lin, W., 2009b. Impacts of air parcel transport on the concentrations of trace gases at regional background stations. J. App. Met. Sci. 20, 656–664 (in Chinese with English abstract).
Xu, W., Lin, W., Xu, X., Tang, J., Huang, J., Wu, H., Zhang, X., 2016. Long-term trends of surface ozone and its influencing factors at the Mt. Waliguan GAW station, China – Part 1: overall trends and characteristics. Atmos. Chem. Phys. 16, 6191–6205. http://dx.doi.org/10.5194/acp-16-6191-2016.
Xue, L.K., Wang, T., Zhang, J.M., Zhang, X.C., Deliger, C.N., Ding, A.J., Zhou, X.H., Wu, W.S., Tang, J., Zhang, Q.Z., Wang, W.X., 2011. Source of surface ozone and reactive nitrogen speciation at Mount Waliguan in western China: new insights from the 2006 summer study. J. Geophys. Res. 116, D07306. http://dx.doi.org/10.1029/2010jd014735.
Xue, L., Wang, T., Louie, P.K.K., Luk, C.W.Y., Blake, D.R., Xu, Z., 2014. Increasing external effects negate local efforts to control ozone air pollution: a case study of Hong Kong and implications for other Chinese cities. Environ. Sci. Technol.

48, 10769–10775. http://dx.doi.org/10.1021/es503278g.
Zeng, G., Pyle, J.A., Young, P.J., 2008. Impact of climate change on tropospheric ozone and its global budgets. Atmos. Chem. Phys. 8, 369–387. http://dx.doi.org/10.5194/acp-8-369-2008.
Zhao, B., Wang, S.X., Liu, H., Xu, J.Y., Fu, K., Klimont, Z., Hao, J.M., He, K.B., Cofala, J., Amann, M., 2013. $NO_x$ emissions in China: historical trends and future perspectives. Atmos. Chem. Phys. 13, 9869–9897. http://dx.doi.org/10.5194/acp-13-9869-2013.
Zhu, B., Akimoto, H., Wang, Z., Sudo, K., Tang, J., Uno, I., 2004. Why does surface ozone peak in summertime at Waliguan? Geophys. Res. Lett. 31, L17104. http://dx.doi.org/10.1029/2004GL020609.